https://doi.org/10.5194/acp-2022-565
Preprint. Discussion started: 22 September 2022

Atmospheric Chemistry and Physics
Discussions

Measurement Report: Year-to-year Variability and Influence of Winter Olympics and other Special Events on Air Quality in Urban Beijing during Wintertime

Yishuo Guo[1,2,★], Chenjuan Deng[3,2,★], Aino Ovaska[2], Feixue Zheng[1], Chenjie Hua[1], Junlei Zhan[1], Yiran Li[3], Jin Wu[3], Zongcheng Wang[1], Jiali Xie[1], Ying Zhang[1], Tingyu Liu[1], Yusheng Zhang[1], Boying Song[1], Wei Ma[1], Yongchun Liu[1], Chao Yan[4,1,2], Jingkun Jiang[3], Veli-Matti Kerminen[2], Men Xia[2,1], Tuomo Nieminen[2], Wei Du[2,1,*], Tom Kokkonen[2,1,4,*], Markku Kulmala[1,2]

[1] Aerosol and Haze Laboratory, Beijing Advanced Innovation Center for Soft Matter Science and Engineering, Beijing University of Chemical Technology, Beijing, China

[2] Institute for Atmospheric and Earth System Research / Physics, Faculty of Science, University of Helsinki, Finland

[3] State Key Joint Laboratory of Environment Simulation and Pollution Control, State Environmental Protection Key Laboratory of Sources and Control of Air Pollution Complex, School of Environment, Tsinghua University, Beijing, China

[4] Joint International Research Laboratory of Atmospheric and Earth System Research, School of Atmospheric Sciences, Nanjing University, Nanjing, China

★ These authors contributed equally to this work.

* *Correspondence to:* Wei Du (wei.du@helsinki.fi) and Tom Kokkonen (tom.kokkonen@helsinki.fi)

Abstract. Comprehensive measurements are vital to obtain big enough datasets for better understanding the complex atmosphere and further improving the air quality. To investigate the year-to-year variabilities of air quality and influences of special events (Beijing Winter Olympics, COVID lockdown and Chinese New Year) on it during the wintertime in a polluted urban air, we conducted comprehensive observations in Beijing, China, during January 1st – February 20th, in the years from 2019 to 2022. The mass concentration of $PM_{2.5}$ and its composition (organics, nitrate, sulfate, ammonium, chloride and black carbon), number size distributions of particles (down to ~1 nm) and ions, gaseous pollutants (CO, NO_x, SO_2, O_3), condensable vapors (sulfuric acid and oxygenated organic molecules), as well as meteorological parameters were simultaneously measured. We selected the period before January 22nd without any special events in each year to show the year-to-year variabilities of the air quality. We found that the concentrations of $PM_{2.5}$, black carbon, chloride, organics, CO, NO_x, total oxygenated organic molecules and number concentration of sub-3 nm particles showed similar year-to-year variabilities, decreasing from 2019 to 2021 and then increasing in 2022. On the contrary, SO_2 concentrations decreased year by year due to the significant emission reduction, leading to decreasing mass concentrations of sulfate and number concentration of sulfuric acid monomer and dimer from 2019 to 2022. As for the influence of special events, due to the favorable meteorological conditions together with reductions in anthropogenic emissions, there were basically no haze events during Beijing Winter Olympics. Although there was emission reduction also during the COVID lockdown period, especially for NO_x, the enhancement of secondary inorganic aerosol formation, together with unfavorable meteorological conditions, caused severe haze events during this period. Additionally, these special events had only little impacts on the new particle formation processes. These results provide useful information to the development of more targeted pollution control plans.

https://doi.org/10.5194/acp-2022-565
Preprint. Discussion started: 22 September 2022

1. Introduction

Beijing and the surrounding areas suffer from poor air quality associated with high particulate matter (PM) concentrations, especially during wintertime. To improve the air quality, extensive studies have been carried out to understand the sources, formation and evolution of air pollutants in Beijing (An et al., 2019; Cheng et al., 2016; Shang et al., 2020; Sun et al., 2014; Zheng et al., 2015). Primary emission sources, including traffic, cooking, coal combustion and biomass burning, have been identified (Cai et al., 2020; Du et al., 2022b; Liu et al., 2016b). Of primary emissions, those from combustions were found to be the major contributors to haze, especially during the heating season (Cheng et al., 2013; Sun et al., 2014; Sun et al., 2013b).

Compared with primary emissions, secondary aerosols have been shown to play a more important role on haze formation, with contributions higher than 60% of PM_1 mass concentration in Beijing (Huang et al., 2014; Kulmala et al., 2022; Shang et al., 2020). Secondary organic aerosols (SOA), nitrate (NO_3) and sulfate (SO_4) originate from their gaseous precursors, e.g., volatile organic compounds (VOCs), nitrogen oxides (NO_x), and sulfur dioxide (SO_2). VOCs, NO_x, and SO_2 further produce oxygenated organic molecules (OOMs), nitric acid (HNO_3), and sulfuric acid (H_2SO_4), respectively, via homogeneous reactions, which can contribute to particle growth by condensation (Bianchi et al., 2019; Trostl et al., 2016; Wang et al., 2020b; Yue et al., 2010). Most recently, Nie et al. (2022) reported that the condensation of OOMs contributed to >30% of SOA in Beijing. Meanwhile, heterogeneous reactions were found to promote the formation of secondary aerosols. Dissolved SO_2 can be oxidized into SO_4 by atmospheric oxidants, e.g., H_2O_2, O_3, and NO_2 (Cheng et al., 2016; Wang et al., 2020a; Zhang et al., 2015). Heterogeneous reactions between HNO_3 and NH_3 in daytime, and hydrolysis of N_2O_5 during night-time are the main pathways forming NO_3 (Wang et al., 2017; Xue et al., 2014). Furthermore, liquid-phase related SOA were found to increase during severe haze when relatively humidity was high (Xu et al., 2017; Zhao et al., 2019). These results highlight the importance of reducing, not only the primary particulate emissions, but also the anthropogenic gaseous precursors to suppress secondary aerosol formation in regional scales (Du et al., 2021; Kulmala et al., 2021).

Regional transport and meteorological conditions also play roles on the evolution of haze episodes. Air masses coming from the south of Beijing often bring pollutants to this area, and hence favor the rapid built up of particle masses (Ma et al., 2017; Sun et al., 2015; Zheng et al., 2015). It has been found that 40% of $PM_{2.5}$ could originate from regional transport in an annual scale (Ge et al., 2018), and under very unfavorable meteorological conditions, it could contribute even up to 80% of the total particle mass during a single haze episode (Sun et al., 2016). Besides, haze events occur typically under stagnant conditions (Zheng et al., 2015). Under such circumstance, high aerosol concentrations tend to delay the onset of precipitation (Guo et al., 2016), and thus, the relative humidity (RH) within the boundary layer is often rather high, which further promotes the heterogeneous reactions producing secondary aerosols (Sun et al., 2013a). Additionally, results have shown that when RH increased above 60%, particles were found to be in a liquid state, thereby accelerating secondary formation (Liu et al., 2017).

The air quality in Beijing has improved substantially over the past decade, especially after introducing the "Action Plan for Air Pollution Prevention and Control" in 2013 (Li et al., 2020b; Lu et al., 2020; Wang et al., 2020d). However, the particulate pollution in Beijing still exceeds the national air quality standards (Xiao et al., 2020). Besides, although the concentration of SO_2 decreased significantly, the level of NO_x remains still high, which results in NO_3 becoming the main contributor of secondary inorganic aerosols (SIA) (Xie et al., 2020). Furthermore, concurrent with the decreasing PM concentrations, ozone is rapidly becoming a year-round air pollution problem in China (Li et al., 2021).

https://doi.org/10.5194/acp-2022-565
Preprint. Discussion started: 22 September 2022

Atmospheric Chemistry and Physics Discussions

In addition to long-term actions, Beijing has imposed strict short-term emission reductions during highly visible international events, such as Beijing Summer Olympics in 2008 (Wang et al., 2010), Asia – Pacific Economic Conference (APEC) in 2014 (Chen et al., 2015; Sun et al., 2016), and Victory Day Parade in 2015 (Zhao et al., 2017). More recently, after the start of the COVID-19 outbreak, the Chinese government carried out strong restrictions (COVID lockdown) in order to prevent the spread of virus. Reduced anthropogenic activities resulted in decreased emissions, yet severe pollution episodes were still observed (Le et al., 2020). In preparation for the Beijing Winter Olympics, the Chinese government authorized necessary actions, successfully improving air quality during this period. Additionally, annual Chinese New Year celebrations are typically associated with reductions in anthropogenic emissions during the 7-day holiday.

All those special events mentioned above have different characteristics in regard to emission reductions. During the COVID lockdown, traffic was reduced, but cooking emissions and industrial activities continued at least partially (Shi and Brasseur, 2020). During the Beijing Winter Olympics, heavy industrial activities were regulated to improve the air quality. During the Chinese New Year, a large proportion of Beijing migrant workers and students from other cities are leaving the city and returning to their hometown. Therefore, anthropogenic emissions from e.g., traffic, cooking and industry are reduced substantially. Thus, a comparison between COVID lockdown, Beijing Winter Olympics and Chinese New Year can provide a unique chance to investigate the response of air pollutants to different emission reduction actions.

In this study, we examined the wintertime (1st January to 20th February) air quality in urban Beijing during a four-year period from 2019 to 2022. We utilised comprehensive observations of air pollutants in both gas phase (including carbon monoxide, sulfur dioxide, nitrogen oxides, ozone, sulfuric acid, and oxygenated organic molecules) and particle phase (including number size distributions of particles and ions, mass concentrations of $PM_{2.5}$ and its compositions), as well as of meteorological conditions (including temperature, RH, UVB radiation, wind speed and direction, and boundary layer height) from Aerosol and Haze Laboratory operated by Beijing University of Chemical Technology (AHL-BUCT; Liu et al., 2020). The objectives of this study are 1) to investigate the year-to-year variabilities of different pollutants and to understand their connections with emissions and meteorological conditions, and 2) to examine the characteristics of atmospheric pollution cocktail during different short-term special events (Beijing Winter Olympics, COVID lockdown and Chinese New Year periods) associated with substantial emission reductions. This study provides helpful information on pollution characteristics of urban Beijing both in a long-term scale and short-term special periods with different emission reductions, which can give guidance to make targeted and sustainable emission control plans.

2. Measurements and methods

2.1 Site description

Beijing is located in the northwestern part of the North China Plain. There are two mountains and a sea nearby. The Taihang Mountain is to the west and the Yanshan Mountain is to the northwest of Beijing, and the nearest Bohai Sea is ~ 150 km to the east. On the south of Beijing, there are several megacities, such as Baoding and Shijiazhuang. Our measurements were conducted at downtown Beijing, the west campus of Beijing University of Chemical Technology (39.95° N, 116.31° E). The instruments are located on the fifth floor of a teaching building, which is ~ 20 m above the ground level. The station can be

https://doi.org/10.5194/acp-2022-565
Preprint. Discussion started: 22 September 2022

Atmospheric Chemistry and Physics Discussions

considered as a representative urban site, and more detailed information can be found elsewhere (Du et al., 2022a; Guo et al., 2021; Liu et al., 2020; Yan et al., 2021).

2.2 Instrumentation

Meteorological variables were measured with a weather station (AWS310, Vaisala Inc.) located on the rooftop of the building. The boundary layer height (BLH) was measured using a ceilometer (CL51, Vaisala). Mixing ratios of trace gases, including carbon monoxide (CO), sulfur dioxide (SO_2), nitrogen oxides (NO_x) and ozone (O_3), were monitored using Thermo Environmental Instruments (models 48i, 43i-TLE, 42i, 49i, respectively).

The concentrations of neutral sulfuric acid (SA) and oxygenated organic molecules (OOMs) were measured by a chemical ionization atmospheric pressure interface long-time-of-flight (CI-APi-TOF, Aerodyne Research, Inc.) mass spectrometers using nitrate (NO_3^-) as the reagent ion. Detailed configurations and working parameters of this nitrate CIMS can be found elsewhere (Guo et al., 2022; Yan et al., 2022). The calibration of SA was implemented by introducing a known amount of gaseous SA produced by the reaction of SO_2 and OH radical formed by UV photolysis of water vapor, which is similar to the method in previous literatures (Kürten et al., 2012). The calibration factor of sulfuric acid was 6.07 – 7.47 $\times 10^9$ cm^{-3} / (normalized cps) from 2019 to 2022. For the quantification of OOMs, a mass-dependent transmission method was used and details of this approach is described elsewhere (Heinritzi et al., 2016). The concentration of each molecular OOM species is calculated as follows:

$$[\mathrm{OOM}] = \frac{\sum_{i=0}^{1}(\mathrm{OOM})(\mathrm{HNO_3})_i\mathrm{NO_3^-} + (\mathrm{OOM-H})^-(\mathrm{HNO_3})_i}{\sum_{i=0}^{2}(\mathrm{HNO_3})_i\mathrm{NO_3^-}} \times \mathrm{C} \div \mathrm{T_{OOM}} \qquad (1)$$

where [OOM] is the concentration of one specific OOM molecule, the numerator on the right-hand side is the sum of detected signal of that OOM, either as neutral molecule or as de-protonated ion $(OOM\text{-}H)^-$, the denominator is the sum of all measured reagent ions, C is the calibration factor of H_2SO_4 and T_{OOM} is the relative transmission coefficient.

The mass concentration of $PM_{2.5}$ was measured with a Tapered Element Oscillating Microbalance Dichotomous Ambient Particulate Monitor (TEOM 1405-DF, Thermo Fisher Scientific Inc, USA). Black carbon (BC) in $PM_{2.5}$ was measured using a seven-wavelength Aethalometer (AE33, Magee Scientific Crop.) (Drinovec et al., 2015). The non-refractory chemical compositions of fine particles (NR-$PM_{2.5}$), including organics (Org), sulfate (SO_4), nitrate (NO_3), ammonium (NH_4), and chloride (Chl), were measured using an online Time-of-Flight Aerosol Chemical Speciation Monitor (ToF-ACSM, Aerodyne Research Inc. U.S.) equipped with a $PM_{2.5}$ aerodynamic lens and a standard vaporizer (Cai et al., 2020; Drewnick et al., 2005; Jayne et al., 2000).

Concerning particle number size distributions, particles in the size range of 1 nm - 10 μm were measured using a diethylene glycol scanning mobility particle spectrometer (DEG-SMPS, 1-7.5 nm) (Jiang et al., 2011; Cai et al., 2017) and a particle size distribution system (PSD, 3 nm-10 μm) (Deng et al., 2020; Liu et al., 2016a; Yan et al., 2021). Based on this particle distribution information, the condensation sink (CS) (Kulmala et al., 2005) of sulfuric acid was then calculated according to method proposed by Kulmala et al. (2012). Additionally, a neutral cluster and air ion spectrometer (NAIS, model 4-11, Airel, Estonia) was used to detect ions in the size range of 0.7–42 nm (mobility diameter) and particles in the size range of 2.5–42 nm (mobility diameter) (Manninen et al., 2016; Mirme and Mirme, 2013; Zhou et al., 2020).

https://doi.org/10.5194/acp-2022-565
Preprint. Discussion started: 22 September 2022

2.3 Calculation of averaged oxygen and nitrogen numbers of total OOMs

The fraction weighted oxygen and nitrogen numbers of OOMs are calculated based on the following equations:

$$\mathrm{nO}(t) = \sum_{i=1}^{n} \mathrm{nO}_i \times Fraction_i(t) \qquad (2)$$

$$\mathrm{nN}(t) = \sum_{i=1}^{n} \mathrm{nN_i} \times Fraction_i(t) \qquad (3)$$

where *n* is the number of OOM molecules, *i* is one specific OOM molecule, nO_i (nN_i) is the number of oxygen (nitrogen) in OOM_i, $Fraction_i$ is the number fraction that OOM_i takes, and t is one certain moment. Then, nO and nN could reflect the averaged oxygen and nitrogen number of total OOMs at each moment. Here, we use nO to generally reflect the oxidation state of total OOMs, and the higher of the nO, the more oxidized of total OOMs.

2.4 Division of different periods

In this study, we focus on the year-to-year variability of air quality in winter Beijing (abbreviated as year-to-year variability in the following text), as well as the influence of special events, including the Beijing Winter Olympics (Olympics), COVID lockdown (COVID) and Chinese New Year (CNY) during the four years from 2019 to 2022. Thus, the whole winter period from 1st January to 20th February was divided into two separated ones (**Fig. S1** and **Table 1**):

a. The periods of year-to-year variability. When the year-to-year variability is investigated, there should be no disturbance from any of the special events, and the chosen days should be from the same periods of different years. Therefore, the period of year-to-year variability covered days from 1st to 22nd January of each year, lasting for 22 days.

b. The periods of special events. To ensure comparable durations for special events, days ranging from 4th to 20th February were chosen as the special event periods. The days within this date range in 2020 and 2022 are referred to as COVID and Olympics periods, respectively. Since CNY holidays in 2022 interfered with Olympics, only CNY holidays in 2019 and 2021 were used and combined together as the CNY period. Finally, for a better understanding of the special event effect, a Reference period including the non-event days in 2019 and 2021 was chosen as the "base-period".

3. Results and discussion

3.1 Year-to-year variability of air quality

3.1.1 Meteorological conditions

Meteorological conditions are strongly interlinked with air quality. Therefore, we first focus on the year-to-year variability of meteorological parameters. As shown in **Fig. 1**, the local wind distributions in 2019 and 2020 were quite similar, following the typical diurnal wind pattern in Beijing induced by the mountain-valley breeze. During the night and morning, the wind mainly blew from the northwest, and the median wind speed (WS) was quite low (~ 0.5 m s^{-1}). From afternoon, however, the wind direction turned to a southerly wind. In 2021, the wind was mostly from the northwest without a clear diurnal variation. In 2022, the wind blew mostly from the southeast during night and morning but came from northeast during afternoon and evening.

https://doi.org/10.5194/acp-2022-565
Preprint. Discussion started: 22 September 2022

Usually, the air masses coming from the south or east possess higher temperatures and bring more water vapor as well as pollutants, whereas air masses coming from the north or west are typically colder with a lower RH and lower pollutant concentrations (Wang et al., 2013; Zhong et al., 2018). The median temperature in 2021 was the lowest (-2.0 °C, **Fig. 2a**) and the median RH was also lower (24 %, **Fig. 2b**) compared with the other three years, which might be partly due to winds coming mainly from northwest throughout the day. The median wind speed in 2021 was also slightly higher (0.75 m s^{-1}, **Fig. 2d**) and the interquartile range had slightly larger range throughout the day than in the other years. As the typical diurnal pattern of wind direction in Beijing is induced by the mountain-valley breeze which is usually occurring only during rather stagnant synoptic conditions, the lack of diurnal pattern of wind direction and the higher wind speeds in 2021 suggest that the synoptic meteorological conditions might have been stronger during this period in 2021 than in the other years. The BLH in 2021 was also the highest throughout the day (**Fig. 2e, f**). During the other three years, the overall values of the temperature, wind speed and BLH were comparable to each other, even though the RH showed signs of an increasing pattern. Higher values of RH may facilitate the hygroscopic growth of aerosol particles (Cheng et al., 2016; Hodas et al., 2014) and change the particle phase state, thereby likely promoting the secondary aerosol formation via heterogeneous reactions (Chao et al., 2020; Hung et al., 2016; Shiraiwa et al., 2017; Sun et al., 2018).

3.1.2 Trace gases

The concentrations of CO, NO and NO_2 decreased from 2019 to 2021 and rebounded in 2022, resulting in their lowest concentrations in 2021 (**Fig. 3**, median values are 308, 5.5, and 12.8 ppb for CO, NO and NO_2, respectively). The variations of CO, NO and NO_2 were generally opposite to that of the BLH, suggesting that atmospheric diffusion capacity could play some role. However, the variation of BLH alone was not enough to explain the huge drops of these pollutants in 2021. In urban Beijing, the sources of NO and NO_2 are mainly vehicle emissions, and thus, the observed variations indicate that the traffic emissions reduced significantly in 2021 and rebounded to some extent in 2022. This is likely associated with the recovery of social activities during the Post COVID-19 Period. For SO_2, a monotonic decrease from 2019 to 2022 was observed, which is consistent with the long-term variation of SO_2 in China, where SO_2 decreased from 24.8 ppb in 2013 to 8.0 ppb in 2017 for the Beijing-Tianjin-Hebei area after the clean air action in 2013 (Wang et al., 2020d;Li et al., 2020). Consequently, our results show that Beijing was successful in the reduction of SO_2, while some challenges still exist in the restriction of NO_x. The year-to-year variability of O_3 was generally opposite to CO and NO_2, and its concentration was the highest in 2021 (15.4 ppb, **Fig. 3d**). This highest O_3 could be partly associated with the weakened titration effect of NO. Meanwhile, the level of O_3 decreased with the increase of $PM_{2.5}$ (**Fig. S6**), suggesting that O_3 formation might be suppressed during haze episodes within the studied period.

3.1.3 Condensable vapors

SA is a key contributor to the formation and initial growth of aerosol particles (Kirkby et al., 2011; Paasonen et al., 2010; Sipilä et al., 2010; Yan et al., 2021; Yao et al., 2018), and OOMs are the main drivers of the particle growth and formation of secondary organic aerosol (SOA) (Ehn et al., 2014; Nie et al., 2022). Therefore, for further investigation of number size distributions and mass concentrations of particles, the year-to-year variabilities of SA and OOMs were first analyzed. As shown in **Fig. 4**, the concentrations of sulfuric acid monomer (SA1, $4.5 - 9.6 \times 10^5$ cm^{-3}, **Fig. 4a**) and dimer (SA2, $3.1 \times 10^3 - 2.8 \times 10^4$ cm^{-3}, **Fig. 4b**) generally decreased from 2019 to 2022. This decreasing trend is similar to that of SO_2, and therefore, the decline of SA1

https://doi.org/10.5194/acp-2022-565
Preprint. Discussion started: 22 September 2022

and SA2 was probably mainly caused by the drop of the precursor SO_2. Additionally, SA2 in 2021 was higher than 2020 and 2022. **Fig. 5** shows that although the data points in 2021 stand out in the SA2 vs. SA1 plot, they lie together with the data points of the other three years in the SA2 vs. $[SA1]^2/CS$ plot. Thus, the elevated SA2 in 2021 was likely caused by the low-level CS (**Fig. S4**).

The year-to-year variability of the total OOM concentration was opposite to that of the BLH. Furthermore, the median OOM concentration in 2019 (2.4×10^7 cm^{-3}) was ~ 8.6 times of that in 2021 (2.8×10^6 cm^{-3}) (**Fig. 4c**), while BLH was lower throughout the day (**Fig. 2f**) and based on the 95th percentile from **Fig. 2e**, the daytime peak BLH in 2019 (~940 m) was only ~0.8 times of that in 2021 (~1200 m). Thus, the reasons behind this drastic yearly change of the OOM concentration are rather complex, and may include the transportation and accumulation of precursor VOCs, change in oxidant concentrations and enhancements of heterogeneous reactions during haze episodes when the BLH is low. Additionally, the total OOM concentrations at same $PM_{2.5}$ levels generally decreased from 2019 to 2022 (**Fig. S7**), suggesting that the condensational growth of OOMs forming SOA under the same $PM_{2.5}$ level likely decreased too. In terms of the OOM composition, **Fig. 4d** shows that the oxygen content of OOMs increased year by year, indicating that the averaged oxidation state of OOMs was enhanced gradually. This might be caused by the elevation of atmospheric oxidation capacity, however evidence on that is lacking at this moment and further investigations are highly needed. Also, the nitrogen content of OOMs increased from 2019 to 2022, suggesting that the involvement of NO_x in OOM formation was enhanced. The change of median nN value from 2019 to 2022 was 0.17, and this increasing trend may continue in the future as the NO_x to VOCs ratios will likely increase due to the fact that the decrease of NO_x is slower than that of VOCs (Li et al., 2020b; Yao et al., 2022).

3.1.4 Particles and ions

Figure 6 shows the year-to-year variabilities of number concentrations of particles in different size ranges. The number concentration of sub-3 nm particles ($N_{1.3\text{-}3}$) decreased from 2019 to 2021, but increased slightly from 2021 to 2022. The influencing factors behind this variability are discussed in the following text. Number concentrations in the nucleation mode (3-25 nm, $N_{3\text{-}25}$) and Aitken mode (25-100 nm, $N_{25\text{-}100}$), generally decreased from 2019 to 2022. Especially, $N_{3\text{-}25}$ was significantly lower in 2022 than in the other years, which could be attributed to fewer nucleated particles growing into larger sizes when NPF events occurred in 2022 (as shown in **Fig. S2**). In contrast, the OOMs concentration was higher in 2022 than in 2021 (**Fig. 4c**), so reasons for the less efficient grow of the nucleation mode particles in 2022 should be explored further. The accumulation mode particle number concentration ($N_{100\text{-}1000}$) was significantly lower in 2021 than in other years, suggesting a suppressed growth of particles from the Aitken mode to larger sizes in measured air masses. This is consistent with the fact that the wind was mainly from northwest in 2021, bringing clean air with low gaseous precursor concentrations. Thus, the overall low $N_{100\text{-}1000}$ in 2021 could also be associated with the more frequent clean air episodes with $PM_{2.5} \leq 35$ µg cm^{-3} in 2021 (67%, **Fig. S3a**).

The year-to-year variability of $N_{1.3\text{-}3}$ was contributed by several factors associated with both sources and sinks of these particles. In urban Beijing, as reported in previous studies (Cai et al., 2021; Deng et al., 2021; Deng et al., 2020; Du et al., 2022a), the formation and growth of new particles is influenced by the SA concentration, background aerosol population, amine concentration and ambient temperature, among other things. The SA concentration decreased from 2019 to 2022, and the $PM_{2.5}$ mass concentration, which is strongly associated with the coagulation caused by background aerosols, was the lowest in 2021 (**Fig. 9**). Also, as shown in **Fig. 2**, the ambient temperature was the lowest in 2021, causing favorable conditions for the

https://doi.org/10.5194/acp-2022-565
Preprint. Discussion started: 22 September 2022

formation of new particles because small clusters evaporate less efficiently when temperatures are lower. However, with such favorable conditions, the $N_{1.3\text{-}3}$ was still the lowest in 2021. The intensities of NPF events were lower in 2021 than 2022, while the NPF event frequency was higher in 2021. A possible reason for this observation is amines, the concentrations of which could have been reduced in 2021 due to limited traffic emissions (indicated by NO_x). However, the influence of this factor is uncertain without simultaneous measurements. The opposite year-to-year variability of BLH can also partly explain that of $N_{1.3\text{-}3}$.

Unlike the number concentration of sub-3 nm particles, the ion concentrations in both 0.8-2 ($N_{0.8\text{-}2,\ \mathrm{ions}}$) and 2-4 nm ($N_{2\text{-}4,\ \mathrm{ions}}$) size ranges were higher in 2021 than in the other years (**Fig. 7**), possibly due to variations in ion source strengths. The ion concentration was higher in the size range of 0.8-2 nm than in the size range of 2-4 nm, which is consistent with previous studies (Kulmala et al., 2013). **Figure S8** shows the levels of $N_{1.3\text{-}3}$ and $N_{0.8\text{-}2,\ \mathrm{ions}}$ under different pollution level among those four years. We found that $N_{1.3\text{-}3}$ decreased with the increasing $PM_{2.5}$ levels, while sub-2 nm ions showed relatively constant concentrations under different pollution levels. These results suggested that background aerosol particles played a more significant role in scavenging small particles than ions.

Figure 8 shows that there was a positive and relatively strong association between the concentrations of 2-3 nm particles and the concentrations of SA1 and SA2 in every year, probably because the formation and growth of nucleated particles is strongly dependent on SA. A weak positive association was also observed between the 2-4 nm ion concentration and SA1 and SA2 concentration. Since 2-4 nm ions originate from collisions between small ions and particles, their concentration is expected to be correlated with SA2, especially as the concentrations of 2-3 nm particles were strongly correlated with concentrations of SA2.

3.1.5 $PM_{2.5}$ and its compositions

The $PM_{2.5}$ mass concentration generally decreased from 2019 to 2021, while rebounding in 2022 to reach a similar level as in 2020 (**Fig. 9**). In 2019, although the median value was similar to those in 2020 and 2022, the average $PM_{2.5}$ mass concentration was higher than in 2020 and 2022. This is because there were more severe haze events in 2019 ($PM_{2.5}$ > 150 μg cm^{-3}, 7%, **Fig. S3a**), which increased the average $PM_{2.5}$ mass concentration considerably. The lowest $PM_{2.5}$ mass concentration coincides with the highest BLH in 2021 (**Fig. 2e, f**). In addition, winds were mainly from northwest in 2021, bringing clean air masses with low PM loadings, and hence the frequency of $PM_{2.5} \leq 35$ μg cm^{-3} was the highest in 2021 (67%, **Fig. S3**). These results indicate the important influence of meteorological conditions on air quality. $PM_{2.5}$ concentrations are also driven by primary emissions and secondary production, discussed in more detail below.

The mass concentrations of Chl, BC and Org showed similar year-to-year variabilities as the $PM_{2.5}$ mass concentration, with a decrease from 2019 to 2021 and then an increase in 2022 (**Fig. 10**). Related mainly to primary sources, the mass concentrations of Chl and BC had similar year-to-year variabilities as CO, a tracer for combustion sources. The mass concentration of Org had a similar year-to-year variability as Chl and BC, which is because primary emissions like combustions partly contribute to the Org in the particle phase. Another important contributor to Org is secondary formation processes. Previous studies suggest that OOMs, which also decreased from 2019 to 2021 and then increased in 2022, can contribute a substantial fraction to secondary organic aerosol mass concentrations (Nie et al., 2022), Therefore, the year-to-year variability of Org can be attributed to both primary emissions and secondary production processes.

However, unlike Chl, BC and Org, sulfate showed the lowest concentration in 2022. The generally decreasing trend of the sulfate mass concentration is consistent with the decreasing trend of the SO_2 concentration from 2019 to 2022, reflecting the significant reduction of SO_2 emissions that China has made during the recent years.

Nitrate and ammonium had their lowest concentrations in 2021 with an increase in 2022 but, unlike Chl, BC and Org, they had higher concentrations in 2020 than in 2019. The similar year-to-year variabilities of nitrate and ammonium is mainly because ammonium tends to be associated with nitrate and sulfate in the particle phase, and the contribution of nitrate becomes dominant due to the significant reduction of SO_2 emissions. With lower NO_x in 2020 than 2019 (**Fig. 3b, c**), the higher NO_3 concentrations in 2020 than those in 2019 suggest that more nitrogen oxides were transformed into particulate nitrate. **Figure S12** shows that at almost all $PM_{2.5}$ levels, the mass concentration of nitrate in 2020 was higher than that in 2019, while NO_2 and NO concentrations were generally lower in 2020. One possible reason for this is the much higher RH in 2020, leading to more aerosol liquid water content, which promotes the uptake of HNO_3 and the hydrolysis of N_2O_5 (Wang et al., 2020c).

Despite some year-to-year variabilities of the mass fractions of the different aerosol component, Org always contributed the largest fraction to the mass concentration of $PM_{2.5}$ in every year, followed by nitrate (**Fig. 11a**). The nitrate fraction generally increased from 20% in 2019 to 28% in 2022, suggesting the more and more important role of nitrate formation. The important role of the organics and nitrate in the $PM_{2.5}$ composition has also been found in previous studies in Beijing (Hu et al., 2021; Sun et al., 2020; Xu et al., 2019).

Figure 11b shows that when the $PM_{2.5}$ mass concentration increased from smaller than 35 μg m^{-3} to larger than 150 μg m^{-3}, the mass fraction of secondary inorganic aerosol (SIA), including nitrate, sulfate and ammonium, increased while the mass fraction of organics decreased in every year. This phenomenon was mainly driven by the increase of the nitrate fraction. Especially in 2021 and 2022 when the $PM_{2.5}$ mass concentration was between 35 and 150 μg m^{-3}, the mass fraction of nitrate was the largest among the different components. Our results indicate the important role of nitrate to haze formation and the urgent need for significantly reductions in NO_x emissions in order to improve the air quality in Beijing.

A number of studies have investigated the yearly changes of chemical compositions of particulate matter in Beijing in recent years (Hu et al., 2021; Wang et al., 2019; Xu et al., 2019; Zhang et al., 2020; Zhou et al., 2019). Due to the implementation of air quality regulations, most of the compounds in particulate matter have decreased significantly. For example, chloride of PM_1 decreased by 65-89% from 2011-2012 to 2017-2018 in urban Beijing using an ACSM (Zhou et al., 2019). In this study, organics also decreased by 37-70%. However, the nitrate concentration did not decrease but even increased. The nitrate concentration was also found to increase by ~4% during winter time from 2007 to 2017 in a previous study (Zhang et al., 2020). Additionally, many studies found that nitrate gradually becomes the major contributor to the chemical composition of particulate matter, overweighing organics, especially during severe haze periods (Hu et al., 2021; Xu et al., 2019). These results are consistent with ours, indicating the importance of reducing NO_x concentration in Beijing.

3.2 The influence of different special events on air quality

3.2.1 Meteorological conditions

Meteorological conditions were not substantially different among different special events, with a few notable exceptions that might have influence on air quality. There are three meteorological characteristics needed to be mentioned. First, the wind

https://doi.org/10.5194/acp-2022-565
Preprint. Discussion started: 22 September 2022

Atmospheric Chemistry and Physics
Discussions

direction distribution during Reference, CNY and COVID periods were generally similar and followed the typical diurnal wind pattern in Beijing (**Fig. 12a, b, c**). Specifically, during the night and morning, winds mostly blew from northwest and sometimes also from northeast, while from afternoon to early night the wind direction turned to the south or southeast. During Olympics, however, the wind pattern was not as strong as in the other events (**Fig. 12d**). From the mid-night to morning the dominant wind direction was the southwest, instead of northwest as during the other events. While during the afternoon and evening, there was no prevailing wind direction, and in addition to the typical southerly winds, there were also winds from northeast. This feature could have affected the air quality positively during the Olympics as there were less frequent southerly winds which are typically associated with more polluted air masses. Second, the median temperatures during Olympics (-0.6 ℃) and CNY (-0.5 ℃) were lower than during Reference (2.5 ℃) and COVID (2.6 ℃) periods (**Fig. 13a**). The temperature variation may cause changes in the rate of gas- and particle-phase reactions as well as in the volatility of oxygenated organic molecules, and thereby may have slight influence on the air quality. Third, the median RH during the COVID period (52 %) was higher than during the other three periods (24 – 27 %) (**Fig. 13b**). As discussed in Sect. 3.1.1, the high RH levels could promote the secondary aerosol formation through heterogeneous reactions. Meanwhile, the wind speeds (**Fig. 12** and **Fig. 13d**) and BLH levels (**Fig. 13e, f**) during the four periods were comparable to each other, so that the vertical mixing of air masses was likely relatively similar among different periods.

3.2.2 Trace gases

Since the restrictions during the COVID, Olympics and CNY periods aim at different sections of social life and production activities, trace gases may have different responses to different periods. As shown in **Fig. 14**, the concentrations of NO and NO_2 during the three restriction periods were all lower than the Reference period, suggesting that the controlling measures during the COVID, Olympics and CNY were effective in reducing NO_x. Apart from that, other trace gases had variable responses to different special events. First, during COVID, the concentration of CO was extremely high (849 ppb), even exceeding that in the Reference period (571 ppb) (**Fig. 14a**). **Fig. S3b and S10** give us a possible explanation for such behavior, showing that severe haze ($PM_{2.5}$ > 75 μg m^{-3}) occurred with the highest frequency during COVID (47 %) compared with the other three periods (1 – 32 %), and that the CO concentration increased with increasing $PM_{2.5}$. Second, when $PM_{2.5}$ exceeded 35 μg m^{-3}, the SO_2 concentrations during COVID were much lower than during the other periods (**Fig. S10**). This feature was associated with higher values RH (**Fig. S9**) and higher particulate sulfate concentrations (**Fig. S13**). Therefore, the conversion of gaseous SO_2 to particulate sulfate was likely enhanced during COVID when the $PM_{2.5}$ concentration was larger than 35 μg m^{-3}. Third, during Olympics, the mixing ratios of CO and SO_2 were the lowest, which was probably caused by the cleanest air masses during this period (See **Sect. 3.2.1** for corresponding discussions). On the contrary, O_3 had the highest concentration (median value 28.1 ppb, **Fig. 14d**) during Olympics, which could partially be related to the low NO_x concentrations. However, as the level of O_3 is affected by many factors, such as meteorological conditions, regional transport (Ge et al., 2012; Lin et al., 2019; Liu et al., 2019; Zhao et al., 2021), photochemical processes associated with solar radiation, NO_x and VOCs (Li et al., 2020a; Tan et al., 2018), further analysis is highly needed for digging out these causes. Additionally, O_3 and $PM_{2.5}$ showed a non-linear relationship during the special event period (**Fig. S10**). More specifically, O_3 first decreased and then increased with increasing $PM_{2.5}$, which is consistent with previous studies (Wang et al., 2020d; Zhao et al., 2020). As for the CNY period, its restriction effect on NO_x was comparable with Olympics, but not for SO_2 due to fireworks. Overall, our results suggest that the restrictions during Olympics were the most effective in controlling primary gaseous pollutants.

https://doi.org/10.5194/acp-2022-565
Preprint. Discussion started: 22 September 2022

3.2.3 Condensable vapors

The responses of SA and OOMs to the three restriction periods were quite different. For SA, the concentrations of SA1 and SA2 were the lowest during COVID (median value are 4.2×10^5 cm^{-3} and 5.7×10^3 cm^{-3} for SA1 and SA2, respectively) and were comparable in the other three periods (median values are $6.0 – 8.7 \times 10^5$ cm^{-3} and $1.5 – 1.9 \times 10^4$ cm^{-3} for SA1 and SA2, respectively) (**Fig. 15a, b**). Since SA is mainly produced from SO_2 oxidation by OH radicals (Finlayson-Pitts and Pitts Jr., 2000) and is primarily scavenged by condensation onto particles (Dada et al., 2020; Guo et al., 2021; Yang et al., 2021), the lowest concentration during COVID could be attributed to the highest condensation sink (**Fig. S4b**) accompanied by the low SO_2 concentration (**Fig. 14e**). Despite the lowest SO_2 concentrations during Olympics, SA1 was not low (**Fig. 15a**) and SA2 was even the highest (**Fig. 15b**). This was probably caused by the synergistic effects of decreased condensation sink (**Fig. S4b**) and increased atmospheric oxidation capacity during Olympics (which could be partially indicated by the highest O_3, **Fig. 14d**). Meanwhile, compared with COVID and Reference periods, the ratios of SA2/SA1 during Olympics and CNY were higher, suggesting that the cluster formation efficiency of sulfuric acid was enhanced during those two periods.

The concentration of the total OOMs (median values are $1.5 – 2.8 \times 10^7$ cm^{-3}, **Fig. 15d**) was the highest during COVID. Compared with SA, the production and loss processes of OOMs are much more complex: they can be generated from the oxidation of VOCs (volatile organic compounds) and OVOCs (oxygenated volatile organic compounds), or be evaporated from the particle phase (Kohli and Davies, 2021; Wilson et al., 2015; Yli-Juuti et al., 2017). When it comes to the loss processes, OOMs can be consumed by further oxidation processes, or through absorption onto particle surfaces via pure condensation or reactive uptake. Among all these factors, precursor VOCs and OVOCs could have great impacts. Since such precursors tend to come along with pollution (Niu et al., 2022; Yao et al., 2021), OOM concentration also showed a strong association with the pollution level (**Fig. S11**). This is probably why the OOM concentration was the highest during COVID when severe haze ($PM_{2.5}$ > 75 μg m^{-3}) was most frequent, and the lowest during Olympics when there was almost no severe haze (**Fig. 3b**). For OOMs themselves, **Fig. 15** and **Fig. S11** together show that under the same $PM_{2.5}$ level, both the averaged oxygen and nitrogen numbers during Olympics were the highest, which implies that not only the oxidation state of OOMs was enhanced, but also the involvement of NO_x was more effective during Olympics.

3.2.4 Particles and ions

As shown in **Fig. 16**, $N_{1.3\text{-}3}$ was almost at the same level during the Reference, COVID, Olympics, and CNY periods. $N_{3\text{-}25}$ was lower during CNY period and $N_{25\text{-}100}$ were slightly lower during Olympics than during the other periods. However, $N_{100\text{-}1000}$ was significantly lower during Olympics compared with the other periods.

The small variability of $N_{1.3\text{-}3}$ between the different periods indicate that the special events may have only little effect on the formation of sub-3 nm particles, i.e., new particle formation processes, consistent with a previous study (Yan et al., 2022). However, for the accumulation particles, the significantly lower number concentrations during Olympics indicates a great impact of the reduction of anthropogenic emissions on large particles during this period. Also, the frequent wind direction from the north indicates the transport of clean air mass during Olympics.

Ion concentrations in the different size ranges were significantly higher during Olympics compared with the other periods (**Fig. 17**). During COVID, the ion concentrations were the lowest. Such differences between the different periods basically follow the year-to-year variabilities of ion concentrations. As discussed in Sect. 3.1.5, the ion concentrations were higher in 2022 compared with the other years, which is consistent with the higher ion concentrations during Olympics in 2022 than during the COVID, CNY and reference periods.

3.2.5 $PM_{2.5}$ and its compositions

The median mass concentration of $PM_{2.5}$ was the lowest during Olympics and the highest during COVID, as compared with the other periods (**Fig. 18**). During the CNY period, the median mass concentration of $PM_{2.5}$ was the second highest. The differences in the $PM_{2.5}$ mass concentration between the different periods were not due to different values of the BLH, since the BLH was similar between the COVID and Olympics periods and the highest during the CNY period (**Fig. 13e**).

Favorable meteorological conditions for transport of clean air mass during Olympics is one of the main reasons leading to the lowest $PM_{2.5}$ mass concentration. In contrast, unfavorable meteorological conditions during the COVID and CNY periods worsened air quality during these two periods. As shown in **Fig. 12**, the wind cycle was obviously different during Olympics than during the other periods. In urban Beijing surrounded by mountains to its west, north and northeast, there is a typical wind cycle with winds tending to come from north or northwest in the morning and from south or southeast in the evening. Such a cycle was obvious during the CNY and COVID periods, allowing the transport of polluted air masses to urban Beijing from the south or south east, thereby leading to severe haze events.

Another reason for the much lower mass concentrations of $PM_{2.5}$ during Olympics compared with the Reference period were the restriction measures on reducing anthropogenic emissions during this time period. Consistently, there were much lower concentrations of primary particles, i.e., BC and Chl, during Olympics than during the Reference period (**Fig. 19**). Although strict restrictions were also performed during COVID, BC and Chl concentrations were slightly higher than during the Reference period. This should not be interpreted as that emission control was not effective during COVID. In fact, BC during COVID was lower than during the Reference at the same $PM_{2.5}$ levels (**Fig. 13f**). The higher average BC concentration during COVID was associated with the higher frequency of haze episodes during COVID. During CNY, the relatively high primary aerosol concentrations seem to be associated with fireworks.

Secondary aerosol formation is important to understanding $PM_{2.5}$ levels as this process is often the main contributor to the particle mass concentration. The much higher fraction of SIA compared to the other components during COVID (**Fig. 20a**) indicates the enhancement of atmospheric oxidation capacity, which might explain the more severe haze events during this period compared with the other periods. As shown in **Fig. 20b,** the mass fraction of SIA was much higher during COVID, and when the $PM_{2.5}$ mass concentration was higher than 35 μg m^{-3}, the mass fraction of SIA reached almost 70%. The much higher values of RH during COVID could have promoted heterogeneous reactions to produce higher SIA concentrations (**Fig. 13b**). Besides, nitrate showed higher concentrations and mass fractions when $PM_{2.5}$ increased from 35 μg m^{-3} to larger concentrations during COVID than other periods, although there was a reduction in NO_x emissions due to strict restrictions on vehicles this period. This phenomenon indicates that secondary formation of nitrate was enhanced and thus contributed to the formation of haze during COVID. In the case of sulfate, although the SO_2 concentration was low during COVID, the overall mass concentration and mass fraction of sulfate was higher than during the other periods, which might be associated with the much higher values of RH during COVID. With higher mass concentrations and fractions of nitrate and sulfate, the ammonium was correspondingly higher during COVID than during the other periods.

https://doi.org/10.5194/acp-2022-565
Preprint. Discussion started: 22 September 2022

Atmospheric Chemistry and Physics
Discussions

4. Summary and conclusions

This study investigated the air quality in a megacity, Beijing, with an emphasis on the year-to-year variability during wintertime and the influences of special events. Numerous variables, including meteorological parameters, concentrations of trace gases, gaseous sulfuric acid and oxygenated organic molecules, number concentrations of atmospheric particles and ions, as well as $PM_{2.5}$ and its composition, were systematically analyzed. The comprehensive data sets span the dates from 1st January to 20th February in the years from 2019 to 2022.

In the first part, the year-to-year variability of air quality during winter Beijing was explored and the data sets before 23rd January were used. Generally, the meteorological conditions during the four years were similar, except that the air masses in 2021 were much cleaner, with only ~ 6 % heavy-polluted days ($75 < PM_{2.5} \leq 150$ µg m^{-3}) and no severe haze days ($PM_{2.5} > 150$ µg m^{-3}). The highest fraction of clean conditions in 2021 was likely favored by the strongest atmospheric diffusion capacity accompanied by the highest average wind speed and boundary layer height. Most gaseous pollutants (like CO, NO, NO_2, total OOMs) and intensive aerosol variables (like concentrations of sub-3nm particles, $PM_{2.5}$, organic aerosol, chloride and black carbon) decreased from 2019 to 2021 while rebounded in 2022. Such rebound of pollutants in 2022 is likely associated with the recovery of social activities during the Post COVID-19 Period. This suggests that the air quality in urban Beijing was gradually improved, but we should still pay careful attention to control measures since there are still frequent severe haze days occurring. Unlike the variation of the above pollutants, SO_2 monotonically decreased from 2019 (3.06 ppb) to 2022 (0.68 ppb), which is consistent with the restriction of SO_2 emission. The O_3 concentration showed an opposite year-to-year variability compared with NO_x that it increased from 2019 (6.3 ppb) to 2021 (15.4 ppb) and dropped in 2022 (8.1 ppb). Meanwhile, both oxygen and nitrogen contents of gas-phase oxygenated organic molecules increased year by year, implying that not only the oxidation state of those compounds was increased, but also NO_x was involved more efficiently in their formation processes. Owing to the significant emission reduction of SO_2 emissions, concentrations of gaseous sulfuric acid monomer, dimer and particulate sulfate generally decreased from 2019 (9.6×10^5 cm^{-3}, 2.8×10^4 cm^{-3} and 2.2 µg m^{-3} for sulfuric acid monomer, dimer and sulfate respectively) to 2022 (4.5×10^5 cm^{-3}, 3.1×10^3 cm^{-3} and 1.1 µg m^{-3} for sulfuric acid monomer, dimer and sulfate respectively). It was found that with higher sulfuric acid concentrations and NPF frequencies in 2021 than in 2022, and with the lowest concentrations of background aerosols and the lowest ambient temperatures in 2021, $N_{1.3\text{-}3}$ was still the lowest in 2021. This indicates that further studies are needed to explore the reasons behind this phenomenon. Moreover, we found that the contribution of nitrate to PM_1 increased from 20 % in 2019 to 28 % in 2022. The increasing trend of nitrate contribution was more pronounced during polluted conditions (PM > 35 µg m^{-3}), indicating the important role of nitrate to haze formation and the urgent need for significantly reductions in NO_x emissions.

In the second part, the influence of special events, including Chinese New Year, COVID lockdown and Beijing Winter Olympics, was investigated. The control measures during COVID and Olympics were effective in reducing NO_x and SO_2. There was no active emission control during CNY, but rather, "indirect" emission reductions were present due to changes in human behavior. As a result, only NO_x emissions were effectively reduced during CNY. The relationships between the O_3 and $PM_{2.5}$ concentrations were interesting. During the period of year-to-yearly variability, O_3 monotonically declined with increasing $PM_{2.5}$, whereas during the reference, COVID and CNY periods, O_3 first decreased and then increased as the $PM_{2.5}$ levels went up. This suggests that the synergetic control strategy of $PM_{2.5}$ and O_3 should adapt to the seasonality. Beneficial from favorable meteorological conditions and significant reductions in anthropogenic emissions, there were basically no haze events ($PM_{2.5}$ > 75 μg m^{-3}) during Olympics, and the median mass concentration of $PM_{2.5}$ (13.7 μg m^{-3}) was also the lowest, around one-third of that during the Reference period (42.7 μg m^{-3}). However, during the COVID period, although strict emission reductions were conducted, haze events still occurred with the highest frequency (~ 29 % for 75 < $PM_{2.5}$ ≤ 150 μg m^{-3}, and ~ 18 % for $PM_{2.5}$ > 150 μg m^{-3}). The high values of RH during COVID likely facilitated the gas-to-particle conversion of sulfur-containing and nitrogen-containing compounds, resulting in high concentrations of particulate sulfate (8.5 μg m^{-3}), nitrate (16.2 μg m^{-3}) and ammonium (8.6 μg m^{-3}), which were around 6.1, 2.5 and 3.3 times those during the reference period, respectively. Meanwhile, $N_{1.3\text{-}3}$ was almost at the same level during the reference, CNY, COVID and Olympics periods, indicating that the special events may have only little impacts on new particle formation processes. However, $N_{100\text{-}1000}$ was significantly lower during Olympics than other periods, showing the significant reduction of anthropogenic emissions during this period.

These results provide useful information on how air quality is affected by different emission reduction scenarios, which will help in planning more targeted and sustainable long-term pollution control plans.

Data availability: Datasets for this paper can be accessed at https://doi.org/10.5281/zenodo.7100748 (Guo et al., 2022).

Author contributions: Y.G, C.D, T.K., W.D. and M.K. designed the research; Y.G., C.D., F.Z., Y.L., J.W., C.H., J.Z., Z.W., J.J., Y.Z., T.L., Y.Z., B.S., W.M., Y.L., C.Y., J.J., and M.K. collected the data; Y.G., C.D. and A.O. analyzed data with the help from T.K., W.D., T.N., V.K., M.X., C.Y. and M.K.; Y.G., C.D., T.K. and W.D. wrote the paper with inputs from all co-authors.

Competing interests: The author declares no competing interests.

Acknowledgements: We acknowledge the following projects: ACCC Flagship funded by the Academy of Finland grant number 337549; Academy professorship funded by the Academy of Finland (grant no. 302958); Academy of Finland projects no. 1325656, 311932, 316114, 332547, and 325647; "Quantifying carbon sink, CarbonSink+ and their interaction with air quality" INAR project funded by Jane and Aatos Erkko Foundation; European Research Council (ERC) project ATM-GTP Contract No. 742206; "Air pollution cocktail in Gigacity" by The Jenny and Antti Wihuri Foundation. Technical and scientific staff in Beijing, AHL/BUCT laboratory are acknowledged.

https://doi.org/10.5194/acp-2022-565
Preprint. Discussion started: 22 September 2022

References

An, Z., Huang, R. J., Zhang, R., Tie, X., Li, G., Cao, J., Zhou, W., Shi, Z., Han, Y., Gu, Z., and Ji, Y.: Severe haze in northern China: A synergy of anthropogenic emissions and atmospheric processes, Proceedings of the National Academy of Sciences of the United States of America, 116, 8657-8666, 10.1073/pnas.1900125116, 2019.

Bianchi, F., Kurten, T., Riva, M., Mohr, C., Rissanen, M. P., Roldin, P., Berndt, T., Crounse, J. D., Wennberg, P. O., Mentel, T. F., Wildt, J., Junninen, H., Jokinen, T., Kulmala, M., Worsnop, D. R., Thornton, J. A., Donahue, N., Kjaergaard, H. G., and Ehn, M.: Highly Oxygenated Organic Molecules (HOM) from Gas-Phase Autoxidation Involving Peroxy Radicals: A Key Contributor to Atmospheric Aerosol, Chem Rev, 119, 3472-3509, 10.1021/acs.chemrev.8b00395, 2019.

Cai, J., Chu, B., Yao, L., Yan, C., Heikkinen, L. M., Zheng, F., Li, C., Fan, X., Zhang, S., Yang, D., Wang, Y., Kokkonen, T. V., Chan, T., Zhou, Y., Dada, L., Liu, Y., He, H., Paasonen, P., Kujansuu, J. T., Petäjä, T., Mohr, C., Kangasluoma, J., Bianchi, F., Sun, Y., Croteau, P. L., Worsnop, D. R., Kerminen, V.-M., Du, W., Kulmala, M., and Daellenbach, K. R.: Size-segregated particle number and mass concentrations from different emission sources in urban Beijing, Atmospheric Chemistry and Physics, 20, 12721-12740, 10.5194/acp-20-12721-2020, 2020.

Cai, R., Chen, D.-R., Hao, J., and Jiang, J.: A miniature cylindrical differential mobility analyzer for sub-3 nm particle sizing, Journal of Aerosol Science, 106, 111-119, https://doi.org/10.1016/j.jaerosci.2017.01.004, 2017.

Cai, R., Yan, C., Yang, D., Yin, R., Lu, Y., Deng, C., Fu, Y., Ruan, J., Li, X., Kontkanen, J., Zhang, Q., Kangasluoma, J., Ma, Y., Hao, J., Worsnop, D. R., Bianchi, F., Paasonen, P., Kerminen, V.-M., Liu, Y., Wang, L., Zheng, J., Kulmala, M., and Jiang, J.: Sulfuric acid–amine nucleation in urban Beijing, Atmospheric Chemistry and Physics, 21, 2457-2468, 10.5194/acp-21-2457-2021, 2021.

Chao, H.-J., Huang, W.-C., Chen, C.-L., Chou, C. C. K., and Hung, H.-M.: Water Adsorption vs Phase Transition of Aerosols Monitored by a Quartz Crystal Microbalance, ACS Omega, 5, 31858-31866, 10.1021/acsomega.0c04698, 2020.

Chen, C., Sun, Y. L., Xu, W. Q., Du, W., Zhou, L. B., Han, T. T., Wang, Q. Q., Fu, P. Q., Wang, Z. F., Gao, Z. Q., Zhang, Q., and Worsnop, D. R.: Characteristics and sources of submicron aerosols above the urban canopy (260 m) in Beijing, China, during the 2014 APEC summit, Atmospheric Chemistry and Physics, 15, 12879-12895, 10.5194/acp-15-12879-2015, 2015.

Cheng, Y., Engling, G., He, K. B., Duan, F. K., Ma, Y. L., Du, Z. Y., Liu, J. M., Zheng, M., and Weber, R. J.: Biomass burning contribution to Beijing aerosol, Atmospheric Chemistry and Physics, 13, 7765-7781, 10.5194/acp-13-7765-2013, 2013.

Cheng, Y., Zheng, G., Wei, C., Mu, Q., Zheng, B., Wang, Z., Gao, M., Zhang, Q., He, K., Carmichael, G., Pöschl, U., and Su, H.: Reactive nitrogen chemistry in aerosol water as a source of sulfate during haze events in China, Science Advances, 2, e1601530, 10.1126/sciadv.1601530, 2016.

Dada, L., Ylivinkka, I., Baalbaki, R., Li, C., Guo, Y., Yan, C., Yao, L., Sarnela, N., Jokinen, T., Daellenbach, K. R., Yin, R., Deng, C., Chu, B., Nieminen, T., Kontkanen, J., Stolzenburg, D., Sipilä, M., Hussein, T., Paasonen, P., Bianchi, F., Salma, I., Weidinger, T., Pikridas, M., Sciare, J., Jiang, J., Liu, Y., Petäjä, T., Kerminen, V. M., and Kulmala, M.: Sources and sinks driving sulphuric acid concentrations in contrasting environments: implications on proxy calculations, Atmos. Chem. Phys. Discuss., 2020, 1-24, 10.5194/acp-2020-155, 2020.

https://doi.org/10.5194/acp-2022-565
Preprint. Discussion started: 22 September 2022

Atmospheric Chemistry and Physics Discussions

Deng, C., Cai, R., Yan, C., Zheng, J., and Jiang, J.: Formation and growth of sub-3 nm particles in megacities: impact of background aerosols, Faraday Discuss, 226, 348-363, 10.1039/d0fd00083c, 2021.

Deng, C., Fu, Y., Dada, L., Yan, C., Cai, R., Yang, D., Zhou, Y., Yin, R., Lu, Y., Li, X., Qiao, X., Fan, X., Nie, W., Kontkanen, J., Kangasluoma, J., Chu, B., Ding, A., Kerminen, V. M., Paasonen, P., Worsnop, D. R., Bianchi, F., Liu, Y., Zheng, J., Wang, L., Kulmala, M., and Jiang, J.: Seasonal Characteristics of New Particle Formation and Growth in Urban Beijing, Environ Sci Technol, 54, 8547-8557, 10.1021/acs.est.0c00808, 2020.

Drewnick, F., Hings, S. S., DeCarlo, P., Jayne, J. T., Gonin, M., Fuhrer, K., Weimer, S., Jimenez, J. L., Demerjian, K. L., Borrmann, S., and Worsnop, D. R.: A New Time-of-Flight Aerosol Mass Spectrometer (TOF-AMS)—Instrument Description and First Field Deployment, Aerosol Science and Technology, 39, 637-658, 10.1080/02786820500182040, 2005.

Drinovec, L., Močnik, G., Zotter, P., Prévôt, A. S. H., Ruckstuhl, C., Coz, E., Rupakheti, M., Sciare, J., Müller, T., Wiedensohler, A., and Hansen, A. D. A.: The "dual-spot" Aethalometer: an improved measurement of aerosol black carbon with real-time loading compensation, Atmos. Meas. Tech., 8, 1965-1979, 10.5194/amt-8-1965-2015, 2015.

Du, W., Cai, J., Zheng, F., Yan, C., Zhou, Y., Guo, Y., Chu, B., Yao, L., Heikkinen, L. M., Fan, X., Wang, Y., Cai, R., Hakala, S., Chan, T., Kontkanen, J., Tuovinen, S., Petäjä, T., Kangasluoma, J., Bianchi, F., Paasonen, P., Sun, Y., Kerminen, V.-M., Liu, Y., Daellenbach, K. R., Dada, L., and Kulmala, M.: Influence of Aerosol Chemical Composition on Condensation Sink Efficiency and New Particle Formation in Beijing, Environmental Science & Technology Letters, 9, 375-382, 10.1021/acs.estlett.2c00159, 2022a.

Du, W., Dada, L., Zhao, J., Chen, X., Daellenbach, K. R., Xie, C., Wang, W., He, Y., Cai, J., Yao, L., Zhang, Y., Wang, Q., Xu, W., Wang, Y., Tang, G., Cheng, X., Kokkonen, T. V., Zhou, W., Yan, C., Chu, B., Zha, Q., Hakala, S., Kurppa, M., Järvi, L., Liu, Y., Li, Z., Ge, M., Fu, P., Nie, W., Bianchi, F., Petäjä, T., Paasonen, P., Wang, Z., Worsnop, D. R., Kerminen, V.-M., Kulmala, M., and Sun, Y.: A 3D study on the amplification of regional haze and particle growth by local emissions, npj Climate and Atmospheric Science, 4, 10.1038/s41612-020-00156-5, 2021.

Du, W., Wang, W., Liu, R., Wang, Y., Zhang, Y., Zhao, J., Dada, L., Xie, C., Wang, Q., Xu, W., Zhou, W., Zhang, F., Li, Z., Fu, P., Li, J., Kangasluoma, J., Wang, Z., Ge, M., Kulmala, M., and Sun, Y.: Insights into vertical differences of particle number size distributions in winter in Beijing, China, Sci. Total Environ., 802, 10.1016/j.scitotenv.2021.149695, 2022b.

Ehn, M., Thornton, J. A., Kleist, E., Sipilä, M., Junninen, H., Pullinen, I., Springer, M., Rubach, F., Tillmann, R., Lee, B., Lopez-Hilfiker, F., Andres, S., Acir, I.-H., Rissanen, M., Jokinen, T., Schobesberger, S., Kangasluoma, J., Kontkanen, J., Nieminen, T., Kurtén, T., Nielsen, L. B., Jørgensen, S., Kjaergaard, H. G., Canagaratna, M., Maso, M. D., Berndt, T., Petäjä, T., Wahner, A., Kerminen, V.-M., Kulmala, M., Worsnop, D. R., Wildt, J., and Mentel, T. F.: A large source of low-volatility secondary organic aerosol, Nature, 506, 476-479, 10.1038/nature13032, 2014.

Finlayson-Pitts, B. J. and Pitts Jr., J. N.: Chemistry of the Upper and Lower Atmosphere: Theory, Experiments, and Applications, 2000.

Ge, B., Wang, Z., Lin, W., Xu, X., Li, J., Ji, D., and Ma, Z.: Air pollution over the North China Plain and its implication of regional transport: A new sight from the observed evidences, Environmental pollution, 234, 29-38, 10.1016/j.envpol.2017.10.084, 2018.

https://doi.org/10.5194/acp-2022-565
Preprint. Discussion started: 22 September 2022

Ge, B. Z., Xu, X. B., Lin, W. L., Li, J., and Wang, Z. F.: Impact of the regional transport of urban Beijing pollutants on downwind areas in summer: ozone production efficiency analysis, Tellus B: Chemical and Physical Meteorology, 64, 17348, 10.3402/tellusb.v64i0.17348, 2012.

Guo, J., Deng, M., Lee, S. S., Wang, F., Li, Z., Zhai, P., Liu, H., Lv, W., Yao, W., and Li, X.: Delaying precipitation and lightning by air pollution over the Pearl River Delta. Part I: Observational analyses, Journal of Geophysical Research: Atmospheres, 121, 6472-6488, 10.1002/2015jd023257, 2016.

Guo, Y., Yan, C., Li, C., Ma, W., Feng, Z., Zhou, Y., Lin, Z., Dada, L., Stolzenburg, D., Yin, R., Kontkanen, J., Daellenbach, K. R., Kangasluoma, J., Yao, L., Chu, B., Wang, Y., Cai, R., Bianchi, F., Liu, Y., and Kulmala, M.: Formation of nighttime sulfuric acid from the ozonolysis of alkenes in Beijing, Atmos. Chem. Phys., 21, 5499-5511, 10.5194/acp-21-5499-2021, 2021.

Guo, Y., Yan, C., Liu, Y., Qiao, X., Zheng, F., Zhang, Y., Zhou, Y., Li, C., Fan, X., Lin, Z., Feng, Z., Zhang, Y., Zheng, P., Tian, L., Nie, W., Wang, Z., Huang, D., Daellenbach, K. R., Yao, L., Dada, L., Bianchi, F., Jiang, J., Liu, Y., Kerminen, V. M., and Kulmala, M.: Seasonal Variation of Oxygenated Organic Molecules in Urban Beijing and their Contribution to Secondary Organic Aerosol, Atmos. Chem. Phys. Discuss., 2022, 1-33, 10.5194/acp-2022-181, 2022.

Heinritzi, M., Simon, M., Steiner, G., Wagner, A. C., Kuerten, A., Hansel, A., and Curtius, J.: Characterization of the mass-dependent transmission efficiency of a CIMS, Atmospheric Measurement Techniques, 9, 1449-1460, 10.5194/amt-9-1449-2016, 2016.

Hodas, N., Sullivan, A. P., Skog, K., Keutsch, F. N., Collett, J. L., Decesari, S., Facchini, M. C., Carlton, A. G., Laaksonen, A., and Turpin, B. J.: Aerosol Liquid Water Driven by Anthropogenic Nitrate: Implications for Lifetimes of Water-Soluble Organic Gases and Potential for Secondary Organic Aerosol Formation, Environmental Science & Technology, 48, 11127-11136, 10.1021/es5025096, 2014.

Hu, S., Zhao, G., Tan, T., Li, C., Zong, T., Xu, N., Zhu, W., and Hu, M.: Current challenges of improving visibility due to increasing nitrate fraction in PM2.5 during the haze days in Beijing, China, Environ Pollut, 290, 118032, 10.1016/j.envpol.2021.118032, 2021.

Huang, R. J., Zhang, Y., Bozzetti, C., Ho, K. F., Cao, J. J., Han, Y., Daellenbach, K. R., Slowik, J. G., Platt, S. M., Canonaco, F., Zotter, P., Wolf, R., Pieber, S. M., Bruns, E. A., Crippa, M., Ciarelli, G., Piazzalunga, A., Schwikowski, M., Abbaszade, G., Schnelle-Kreis, J., Zimmermann, R., An, Z., Szidat, S., Baltensperger, U., El Haddad, I., and Prevot, A. S.: High secondary aerosol contribution to particulate pollution during haze events in China, Nature, 514, 218-222, 10.1038/nature13774, 2014.

Hung, H.-M., Hsu, C.-H., Lin, W.-T., and Chen, Y.-Q.: A case study of single hygroscopicity parameter and its link to the functional groups and phase transition for urban aerosols in Taipei City, Atmospheric Environment, 132, 240-248, https://doi.org/10.1016/j.atmosenv.2016.03.008, 2016.

Jayne, J. T., Leard, D. C., Zhang, X., Davidovits, P., Smith, K. A., Kolb, C. E., and Worsnop, D. R.: Development of an Aerosol Mass Spectrometer for Size and Composition Analysis of Submicron Particles, Aerosol Science and Technology, 33, 49-70, 10.1080/027868200410840, 2000.

Jiang, J., Chen, M., Kuang, C., Attoui, M., and McMurry, P. H.: Electrical Mobility Spectrometer Using a Diethylene Glycol Condensation Particle Counter for Measurement of Aerosol Size Distributions Down to 1 nm, Aerosol Science and Technology, 45, 510-521, 10.1080/02786826.2010.547538, 2011.

Kirkby, J., Curtius, J., Almeida, J., Dunne, E., Duplissy, J., Ehrhart, S., Franchin, A., Gagne, S., Ickes, L., Kuerten, A., Kupc, A., Metzger, A., Riccobono, F., Rondo, L., Schobesberger, S., Tsagkogeorgas, G., Wimmer, D., Amorim, A., Bianchi, F., Breitenlechner, M., David, A., Dommen, J., Downard, A., Ehn, M., Flagan, R. C., Haider, S., Hansel, A., Hauser, D., Jud, W., Junninen, H., Kreissl, F., Kvashin, A., Laaksonen, A., Lehtipalo, K., Lima, J., Lovejoy, E. R., Makhmutov, V., Mathot, S., Mikkila, J., Minginette, P., Mogo, S., Nieminen, T., Onnela, A., Pereira, P., Petaja, T., Schnitzhofer, R., Seinfeld, J. H., Sipila, M., Stozhkov, Y., Stratmann, F., Tome, A., Vanhanen, J., Viisanen, Y., Vrtala, A., Wagner, P. E., Walther, H., Weingartner, E., Wex, H., Winkler, P. M., Carslaw, K. S., Worsnop, D. R., Baltensperger, U., and Kulmala, M.: Role of sulphuric acid, ammonia and galactic cosmic rays in atmospheric aerosol nucleation, Nature, 476, 429-U477, 10.1038/nature10343, 2011.

Kohli, R. K. and Davies, J. F.: Measuring the Chemical Evolution of Levitated Particles: A Study on the Evaporation of Multicomponent Organic Aerosol, Analytical Chemistry, 93, 12472-12479, 10.1021/acs.analchem.1c02890, 2021.

Kulmala, M.: China's choking cocktail, Nature, 526, 497-499, 10.1038/526497a, 2015.

Kulmala, M., Cai, R., Stolzenburg, D., Zhou, Y., Dada, L., Guo, Y., Yan, C., Petaja, T., Jiang, J., and Kerminen, V. M.: The contribution of new particle formation and subsequent growth to haze formation, Environ Sci Atmos, 2, 352-361, 10.1039/d1ea00096a, 2022.

Kulmala, M., Dada, L., Dällenbach, K., Yan, C., Stolzenburg, D., Kontkanen, J., Ezhova, E., Hakala, S., Tuovinen, S., Kokkonen, T., Kurppa, M., Cai, R., Zhou, Y., Yin, R., Baalbaki, R., Chan, T., Chu, B., Deng, C., Fu, Y., Ge, M., He, H., Heikkinen, L., Junninen, H., Nei, W., Rusanen, A., Vakkari, V., Wang, Y., Wang, L., yao, l., Zheng, J., Kujansuu, J., Kangasluoma, J., Petäjä, T., Paasonen, P., Järvi, L., Worsnop, D., Ding, A., Liu, Y., Jiang, J., Bianchi, F., Yang, G., Liu, Y., Lu, Y., and Kerminen, V.-M.: Is reducing new particle formation a plausible solution to mitigate particulate air pollution in Beijing and other Chinese megacities?, Faraday Discuss., 10.1039/d0fd00078g, 2021.

Kulmala, M., Kontkanen, J., Junninen, H., Lehtipalo, K., Manninen, H. E., Nieminen, T., Petäjä, T., Sipilä, M., Schobesberger, S., Rantala, P., Franchin, A., Jokinen, T., Järvinen, E., Äijälä, M., Kangasluoma, J., Hakala, J., Aalto, P. P., Paasonen, P., Mikkilä, J., Vanhanen, J., Aalto, J., Hakola, H., Makkonen, U., Ruuskanen, T., Mauldin, R. L., 3rd, Duplissy, J., Vehkamäki, H., Bäck, J., Kortelainen, A., Riipinen, I., Kurtén, T., Johnston, M. V., Smith, J. N., Ehn, M., Mentel, T. F., Lehtinen, K. E., Laaksonen, A., Kerminen, V. M., and Worsnop, D. R.: Direct observations of atmospheric aerosol nucleation, Science, 339, 943-946, 10.1126/science.1227385, 2013.

Kulmala, M., Petäjä, T., Mönkkönen, P., Koponen, I. K., Dal Maso, M., Aalto, P. P., Lehtinen, K. E. J., and Kerminen, V. M.: On the growth of nucleation mode particles: source rates of condensable vapor in polluted and clean environments, Atmos. Chem. Phys., 5, 409-416, 10.5194/acp-5-409-2005, 2005.

Kulmala, M., Petaja, T., Nieminen, T., Sipila, M., Manninen, H. E., Lehtipalo, K., Dal Maso, M., Aalto, P. P., Junninen, H., Paasonen, P., Riipinen, I., Lehtinen, K. E., Laaksonen, A., and Kerminen, V. M.: Measurement of the nucleation of atmospheric aerosol particles, Nature Protocols, 7, 1651-1667, 10.1038/nprot.2012.091, 2012.

Kürten, A., Rondo, L., Ehrhart, S., and Curtius, J.: Calibration of a chemical ionization mass spectrometer for the measurement of gaseous sulfuric acid, The Journal of Physical Chemistry A, 116, 6375-6386, 2012.

Le, T., Wang, Y., Liu, L., Yang, J., Yung, Y. L., Li, G., and Seinfeld, J. H.: Unexpected air pollution with marked emission reductions during the COVID-19 outbreak in China, Science, 369, 702-706, 2020.

Li, K., Jacob, D. J., Liao, H., Qiu, Y., Shen, L., Zhai, S., Bates, K. H., Sulprizio, M. P., Song, S., Lu, X., Zhang, Q., Zheng, B., Zhang, Y., Zhang, J., Lee, H. C., and Kuk, S. K.: Ozone pollution in the North China Plain spreading into the late-winter haze season, Proc Natl Acad Sci U S A, 118, 10.1073/pnas.2015797118, 2021.

Li, Q., Su, G., Li, C., Liu, P., Zhao, X., Zhang, C., Sun, X., Mu, Y., Wu, M., Wang, Q., and Sun, B.: An investigation into the role of VOCs in SOA and ozone production in Beijing, China, Science of The Total Environment, 720, 137536, https://doi.org/10.1016/j.scitotenv.2020.137536, 2020a.

Li, W., Shao, L., Wang, W., Li, H., Wang, X., Li, Y., Li, W., Jones, T., and Zhang, D.: Air quality improvement in response to intensified control strategies in Beijing during 2013-2019, The Science of the total environment, 744, 140776, 10.1016/j.scitotenv.2020.140776, 2020b.

Li, X., Zhao, B., Zhou, W., Shi, H., Yin, R., Cai, R., Yang, D., Dallenbach, K., Deng, C., Fu, Y., Qiao, X., Wang, L., Liu, Y., Yan, C., Kulmala, M., Zheng, J., Hao, J., Wang, S., and Jiang, J.: Responses of gaseous sulfuric acid and particulate sulfate to reduced SO2 concentration: A perspective from long-term measurements in Beijing, Science of the Total Environment, 721, 137700, 10.1016/j.scitotenv.2020.137700, 2020.

Lin, X., Yuan, Z., Yang, L., Luo, H., and Li, W.: Impact of Extreme Meteorological Events on Ozone in the Pearl River Delta, China, Aerosol and Air Quality Research, 19, 1307-1324, 10.4209/aaqr.2019.01.0027, 2019.

Liu, H., Zhang, M., Han, X., Li, J., and Chen, L.: Episode analysis of regional contributions to tropospheric ozone in Beijing using a regional air quality model, Atmospheric Environment, 199, 299-312, https://doi.org/10.1016/j.atmosenv.2018.11.044, 2019.

Liu, J., Jiang, J., Zhang, Q., Deng, J., and Hao, J.: A spectrometer for measuring particle size distributions in the range of 3 nm to 10 µm, Frontiers of Environmental Science & Engineering, 10, 63-72, 10.1007/s11783-014-0754-x, 2016a.

Liu, Y., Wu, Z., Wang, Y., Xiao, Y., Gu, F., Zheng, J., Tan, T., Shang, D., Wu, Y., Zeng, L., Hu, M., Bateman, A. P., and Martin, S. T.: Submicrometer Particles Are in the Liquid State during Heavy Haze Episodes in the Urban Atmosphere of Beijing, China, Environmental Science & Technology Letters, 4, 427-432, 10.1021/acs.estlett.7b00352, 2017.

Liu, Y., Yan, C., Feng, Z., Zheng, F., Fan, X., Zhang, Y., Li, C., Zhou, Y., Lin, Z., Guo, Y., Zhang, Y., Ma, L., Zhou, W., Liu, Z., Dada, L., Dällenbach, K., Kontkanen, J., Cai, R., Chan, T., Chu, B., Du, W., Yao, L., Wang, Y., Cai, J., Kangasluoma, J., Kokkonen, T., Kujansuu, J., Rusanen, A., Deng, C., Fu, Y., Yin, R., Li, X., Lu, Y., Liu, Y., Lian, C., Yang, D., Wang, W., Ge, M., Wang, Y., Worsnop, D. R., Junninen, H., He, H., Kerminen, V.-M., Zheng, J., Wang, L., Jiang, J., Petäjä, T., Bianchi, F., and Kulmala, M.: Continuous and comprehensive atmospheric observations in Beijing: a station to understand the complex urban atmospheric environment, Big Earth Data, 4, 295-321, 10.1080/20964471.2020.1798707, 2020.

https://doi.org/10.5194/acp-2022-565
Preprint. Discussion started: 22 September 2022

Liu, Z., Wang, Y., Hu, B., Ji, D., Zhang, J., Wu, F., Wan, X., and Wang, Y.: Source appointment of fine particle number and volume concentration during severe haze pollution in Beijing in January 2013, Environmental science and pollution research international, 23, 6845-6860, 10.1007/s11356-015-5868-6, 2016b.

Lu, X., Zhang, S., Xing, J., Wang, Y., Chen, W., Ding, D., Wu, Y., Wang, S., Duan, L., and Hao, J.: Progress of Air Pollution Control in China and Its Challenges and Opportunities in the Ecological Civilization Era, Engineering, 6, 1423-1431, 10.1016/j.eng.2020.03.014, 2020.

Ma, Q., Wu, Y., Zhang, D., Wang, X., Xia, Y., Liu, X., Tian, P., Han, Z., Xia, X., Wang, Y., and Zhang, R.: Roles of regional transport and heterogeneous reactions in the PM2.5 increase during winter haze episodes in Beijing, Sci. Total Environ., 599-600, 246-253, 10.1016/j.scitotenv.2017.04.193, 2017.

Manninen, H. E., Mirme, S., Mirme, A., Petäjä, T., and Kulmala, M.: How to reliably detect molecular clusters and nucleation mode particles with Neutral cluster and Air Ion Spectrometer (NAIS), Atmos. Meas. Tech., 9, 3577-3605, 10.5194/amt-9-3577-2016, 2016.

Mirme, S. and Mirme, A.: The mathematical principles and design of the NAIS – a spectrometer for the measurement of cluster ion and nanometer aerosol size distributions, Atmos. Meas. Tech., 6, 1061-1071, 10.5194/amt-6-1061-2013, 2013.

Nie, W., Yan, C., Huang, D. D., Wang, Z., Liu, Y., Qiao, X., Guo, Y., Tian, L., Zheng, P., Xu, Z., Li, Y., Xu, Z., Qi, X., Sun, P., Wang, J., Zheng, F., Li, X., Yin, R., Dallenbach, K. R., Bianchi, F., Petäjä, T., Zhang, Y., Wang, M., Schervish, M., Wang, S., Qiao, L., Wang, Q., Zhou, M., Wang, H., Yu, C., Yao, D., Guo, H., Ye, P., Lee, S., Li, Y. J., Liu, Y., Chi, X., Kerminen, V.-M., Ehn, M., Donahue, N. M., Wang, T., Huang, C., Kulmala, M., Worsnop, D., Jiang, J., and Ding, A.: Secondary organic aerosol formed by condensing anthropogenic vapours over China's megacities, Nature Geoscience, 15, 255-261, 10.1038/s41561-022-00922-5, 2022.

Niu, Y., Yan, Y., Chai, J., Zhang, X., Xu, Y., Duan, X., Wu, J., and Peng, L.: Effects of regional transport from different potential pollution areas on volatile organic compounds (VOCs) in Northern Beijing during non-heating and heating periods, Science of The Total Environment, 836, 155465, https://doi.org/10.1016/j.scitotenv.2022.155465, 2022.

Paasonen, P., Nieminen, T., Asmi, E., Manninen, H. E., Petaja, T., Plass-Duelmer, C., Flentje, H., Birmili, W., Wiedensohler, A., Horrak, U., Metzger, A., Hamed, A., Laaksonen, A., Facchini, M. C., Kerminen, V. M., and Kulmala, M.: On the roles of sulphuric acid and low-volatility organic vapours in the initial steps of atmospheric new particle formation, Atmospheric Chemistry and Physics, 10, 11223-11242, 10.5194/acp-10-11223-2010, 2010.

Shang, D., Peng, J., Guo, S., Wu, Z., and Hu, M.: Secondary aerosol formation in winter haze over the Beijing-Tianjin-Hebei Region, China, Frontiers of Environmental Science & Engineering, 15, 10.1007/s11783-020-1326-x, 2020.

Shi, X. and Brasseur, G. P.: The Response in Air Quality to the Reduction of Chinese Economic Activities during the COVID-19 Outbreak, Geophys Res Lett, e2020GL088070, 10.1029/2020GL088070, 2020.

Shiraiwa, M., Li, Y., Tsimpidi, A. P., Karydis, V. A., Berkemeier, T., Pandis, S. N., Lelieveld, J., Koop, T., and Pöschl, U.: Global distribution of particle phase state in atmospheric secondary organic aerosols, Nature Communications, 8, 15002, 10.1038/ncomms15002, 2017.

Sipilä, M., Berndt, T., Petäjä, T., Brus, D., Vanhanen, J., Stratmann, F., Patokoski, J., Mauldin Roy, L., Hyvärinen, A.-P., Lihavainen, H., and Kulmala, M.: The Role of Sulfuric Acid in Atmospheric Nucleation, Science, 327, 1243-1246, 10.1126/science.1180315, 2010.

Sun, J., Liu, L., Xu, L., Wang, Y., Wu, Z., Hu, M., Shi, Z., Li, Y., Zhang, X., Chen, J., and Li, W.: Key Role of Nitrate in Phase Transitions of Urban Particles: Implications of Important Reactive Surfaces for Secondary Aerosol Formation, Journal of Geophysical Research: Atmospheres, 123, 1234-1243, 10.1002/2017jd027264, 2018.

Sun, Y., Jiang, Q., Wang, Z., Fu, P., Li, J., Yang, T., and Yin, Y.: Investigation of the sources and evolution processes of severe haze pollution in Beijing in January 2013, Journal of Geophysical Research, 119, 4380-4398, 10.1002/2014jd021641, 2014.

Sun, Y., Lei, L., Zhou, W., Chen, C., He, Y., Sun, J., Li, Z., Xu, W., Wang, Q., Ji, D., Fu, P., Wang, Z., and Worsnop, D. R.: A chemical cocktail during the COVID-19 outbreak in Beijing, China: Insights from six-year aerosol particle composition measurements during the Chinese New Year holiday, The Science of the total environment, 742, 140739, 10.1016/j.scitotenv.2020.140739, 2020.

Sun, Y., Wang, Z., Fu, P., Jiang, Q., Yang, T., Li, J., and Ge, X.: The impact of relative humidity on aerosol composition and evolution processes during wintertime in Beijing, China, Atmospheric Environment, 77, 927-934, 10.1016/j.atmosenv.2013.06.019, 2013a.

Sun, Y., Wang, Z., Wild, O., Xu, W., Chen, C., Fu, P., Du, W., Zhou, L., Zhang, Q., Han, T., Wang, Q., Pan, X., Zheng, H., Li, J., Guo, X., Liu, J., and Worsnop, D. R.: "APEC Blue": Secondary Aerosol Reductions from Emission Controls in Beijing, Sci Rep, 6, 20668, 10.1038/srep20668, 2016.

Sun, Y. L., Wang, Z. F., Du, W., Zhang, Q., Wang, Q. Q., Fu, P. Q., Pan, X. L., Li, J., Jayne, J., and Worsnop, D. R.: Long-term real-time measurements of aerosol particle composition in Beijing, China: seasonal variations, meteorological effects, and source analysis, Atmospheric Chemistry and Physics, 15, 10149-10165, 10.5194/acp-15-10149-2015, 2015.

Sun, Y. L., Wang, Z. F., Fu, P. Q., Yang, T., Jiang, Q., Dong, H. B., Li, J., and Jia, J. J.: Aerosol composition, sources and processes during wintertime in Beijing, China, Atmospheric Chemistry and Physics, 13, 4577-4592, 10.5194/acp-13-4577-2013, 2013b.

Tan, Z., Lu, K., Dong, H., Hu, M., Li, X., Liu, Y., Lu, S., Shao, M., Su, R., Wang, H., Wu, Y., Wahner, A., and Zhang, Y.: Explicit diagnosis of the local ozone production rate and the ozone-NOx-VOC sensitivities, Science Bulletin, 63, 1067-1076, https://doi.org/10.1016/j.scib.2018.07.001, 2018.

Trostl, J., Chuang, W. K., Gordon, H., Heinritzi, M., Yan, C., Molteni, U., Ahlm, L., Frege, C., Bianchi, F., Wagner, R., Simon, M., Lehtipalo, K., Williamson, C., Craven, J. S., Duplissy, J., Adamov, A., Almeida, J., Bernhammer, A. K., Breitenlechner, M., Brilke, S., Dias, A., Ehrhart, S., Flagan, R. C., Franchin, A., Fuchs, C., Guida, R., Gysel, M., Hansel, A., Hoyle, C. R., Jokinen, T., Junninen, H., Kangasluoma, J., Keskinen, H., Kim, J., Krapf, M., Kurten, A., Laaksonen, A., Lawler, M., Leiminger, M., Mathot, S., Mohler, O., Nieminen, T., Onnela, A., Petaja, T., Piel, F. M., Miettinen, P., Rissanen, M. P., Rondo, L., Sarnela, N., Schobesberger, S., Sengupta, K., Sipila, M., Smith, J. N., Steiner, G., Tome, A., Virtanen, A., Wagner, A. C., Weingartner, E., Wimmer, D., Winkler, P. M., Ye, P., Carslaw, K. S., Curtius, J., Dommen, J., Kirkby, J., Kulmala, M., Riipinen, I., Worsnop,

D. R., Donahue, N. M., and Baltensperger, U.: The role of low-volatility organic compounds in initial particle growth in the atmosphere, Nature, 533, 527-531, 10.1038/nature18271, 2016.

Wang, H., Lu, K., Chen, X., Zhu, Q., Chen, Q., Guo, S., Jiang, M., Li, X., Shang, D., Tan, Z., Wu, Y., Wu, Z., Zou, Q., Zheng, Y., Zeng, L., Zhu, T., Hu, M., and Zhang, Y.: High N2O5 Concentrations Observed in Urban Beijing: Implications of a Large Nitrate Formation Pathway, Environmental Science & Technology Letters, 4, 416-420, 10.1021/acs.estlett.7b00341, 2017.

Wang, J., Li, J., Ye, J., Zhao, J., Wu, Y., Hu, J., Liu, D., Nie, D., Shen, F., Huang, X., Huang, D. D., Ji, D., Sun, X., Xu, W., Guo, J., Song, S., Qin, Y., Liu, P., Turner, J. R., Lee, H. C., Hwang, S., Liao, H., Martin, S. T., Zhang, Q., Chen, M., Sun, Y., Ge, X., and Jacob, D. J.: Fast sulfate formation from oxidation of SO2 by NO2 and HONO observed in Beijing haze, Nature communications, 11, 2844, 10.1038/s41467-020-16683-x, 2020a.

Wang, M., Kong, W., Marten, R., He, X. C., Chen, D., Pfeifer, J., Heitto, A., Kontkanen, J., Dada, L., Kurten, A., Yli-Juuti, T., Manninen, H. E., Amanatidis, S., Amorim, A., Baalbaki, R., Baccarini, A., Bell, D. M., Bertozzi, B., Brakling, S., Brilke, S., Murillo, L. C., Chiu, R., Chu, B., De Menezes, L. P., Duplissy, J., Finkenzeller, H., Carracedo, L. G., Granzin, M., Guida, R., Hansel, A., Hofbauer, V., Krechmer, J., Lehtipalo, K., Lamkaddam, H., Lampimaki, M., Lee, C. P., Makhmutov, V., Marie, G., Mathot, S., Mauldin, R. L., Mentler, B., Muller, T., Onnela, A., Partoll, E., Petaja, T., Philippov, M., Pospisilova, V., Ranjithkumar, A., Rissanen, M., Rorup, B., Scholz, W., Shen, J., Simon, M., Sipila, M., Steiner, G., Stolzenburg, D., Tham, Y. J., Tome, A., Wagner, A. C., Wang, D. S., Wang, Y., Weber, S. K., Winkler, P. M., Wlasits, P. J., Wu, Y., Xiao, M., Ye, Q., Zauner-Wieczorek, M., Zhou, X., Volkamer, R., Riipinen, I., Dommen, J., Curtius, J., Baltensperger, U., Kulmala, M., Worsnop, D. R., Kirkby, J., Seinfeld, J. H., El-Haddad, I., Flagan, R. C., and Donahue, N. M.: Rapid growth of new atmospheric particles by nitric acid and ammonia condensation, Nature, 581, 184-189, 10.1038/s41586-020-2270-4, 2020b.

Wang, S., Zhao, M., Xing, J., Wu, Y., Zhou, Y., Lei, Y., He, K., Fu, L., and Hao, J.: Quantifying the Air Pollutants Emission Reduction during the 2008 Olympic Games in Beijing, Environ. Sci. Technol., 44, 2490-2496, 10.1021/es9028167, 2010.

Wang, Y., Chen, Y., Wu, Z., Shang, D., Bian, Y., Du, Z., Schmitt, S. H., Su, R., Gkatzelis, G. I., Schlag, P., Hohaus, T., Voliotis, A., Lu, K., Zeng, L., Zhao, C., Alfarra, M. R., McFiggans, G., Wiedensohler, A., Kiendler-Scharr, A., Zhang, Y., and Hu, M.: Mutual promotion between aerosol particle liquid water and particulate nitrate enhancement leads to severe nitrate-dominated particulate matter pollution and low visibility, Atmospheric Chemistry and Physics, 20, 2161-2175, 10.5194/acp-20-2161-2020, 2020c.

Wang, Y., Gao, W., Wang, S., Song, T., Gong, Z., Ji, D., Wang, L., Liu, Z., Tang, G., Huo, Y., Tian, S., Li, J., Li, M., Yang, Y., Chu, B., Petäjä, T., Kerminen, V.-M., He, H., Hao, J., Kulmala, M., Wang, Y., and Zhang, Y.: Contrasting trends of PM2.5 and surface-ozone concentrations in China from 2013 to 2017, National Science Review, 7, 1331-1339, 10.1093/nsr/nwaa032, 2020d.

Wang, Y., Wang, Q., Ye, J., Yan, M., Qin, Q., Prévôt, A. S. H., and Cao, J.: A Review of Aerosol Chemical Composition and Sources in Representative Regions of China during Wintertime, Atmosphere, 10, 10.3390/atmos10050277, 2019.

Wang, Z. B., Hu, M., Wu, Z. J., Yue, D. L., He, L. Y., Huang, X. F., Liu, X. G., and Wiedensohler, A.: Long-term measurements of particle number size distributions and the relationships with air mass history and source apportionment in the summer of Beijing, Atmos. Chem. Phys., 13, 10159-10170, 10.5194/acp-13-10159-2013, 2013.

https://doi.org/10.5194/acp-2022-565
Preprint. Discussion started: 22 September 2022

Atmospheric Chemistry and Physics Discussions

Wilson, J., Imre, D., Beránek, J., Shrivastava, M., and Zelenyuk, A.: Evaporation Kinetics of Laboratory-Generated Secondary Organic Aerosols at Elevated Relative Humidity, Environmental Science & Technology, 49, 243-249, 10.1021/es505331d, 2015.

Xiao, C., Chang, M., Guo, P., Gu, M., and Li, Y.: Analysis of air quality characteristics of Beijing-Tianjin-Hebei and its surrounding air pollution transport channel cities in China, J Environ Sci (China), 87, 213-227, 10.1016/j.jes.2019.05.024, 2020.

Xie, Y., Wang, G., Wang, X., Chen, J., Chen, Y., Tang, G., Wang, L., Ge, S., Xue, G., Wang, Y., and Gao, J.: Nitrate-dominated PM_{2.5} and elevation of particle pH observed in urban Beijing during the winter of 2017, Atmospheric Chemistry and Physics, 20, 5019-5033, 10.5194/acp-20-5019-2020, 2020.

Xu, Q., Wang, S., Jiang, J., Bhattarai, N., Li, X., Chang, X., Qiu, X., Zheng, M., Hua, Y., and Hao, J.: Nitrate dominates the chemical composition of PM2.5 during haze event in Beijing, China, Sci Total Environ, 689, 1293-1303, 10.1016/j.scitotenv.2019.06.294, 2019.

Xu, W. Q., Han, T. T., Du, W., Wang, Q. Q., Chen, C., Zhao, J., Zhang, Y. J., Li, J., Fu, P. Q., Wang, Z. F., Worsnop, D. R., and Sun, Y. L.: Effects of Aqueous-Phase and Photochemical Processing on Secondary Organic Aerosol Formation and Evolution in Beijing, China, Environ. Sci. Technol., 51, 762-770, 10.1021/acs.est.6b04498, 2017.

Xue, J., Yuan, Z. B., Lau, A. K. H., and Yu, J. Z.: Insights into factors affecting nitrate in PM2.5 in a polluted high NOx environment through hourly observations and size distribution measurements, J. Geophys. Res.-Atmos., 119, 4888-4902, 10.1002/2013jd021108, 2014.

Yan, C., Shen, Y., Stolzenburg, D., Dada, L., Qi, X., Hakala, S., Sundström, A. M., Guo, Y., Lipponen, A., Kokkonen, T., Kontkanen, J., Cai, R., Cai, J., Chan, T., Chen, L., Chu, B., Deng, C., Du, W., Fan, X., He, X. C., Kangasluoma, J., Kujansuu, J., Kurppa, M., Li, C., Li, Y., Lin, Z., Liu, Y., Liu, Y., Lu, Y., Nie, W., Pulliainen, J., Qiao, X., Wang, Y., Wen, Y., Wu, Y., Yang, G., Yao, L., Yin, R., Zhang, G., Zhang, S., Zheng, F., Zhou, Y., Arola, A., Tamminen, J., Paasonen, P., Sun, Y., Wang, L., Donahue, N. M., Liu, Y., Bianchi, F., Daellenbach, K. R., Worsnop, D. R., Kerminen, V. M., Petäjä, T., Ding, A., Jiang, J., and Kulmala, M.: The effect of COVID-19 restrictions on atmospheric new particle formation in Beijing, Atmos. Chem. Phys. Discuss., 2022, 1-24, 10.5194/acp-2021-1079, 2022.

Yan, C., Yin, R., Lu, Y., Dada, L., Yang, D., Fu, Y., Kontkanen, J., Deng, C., Garmash, O., Ruan, J., Baalbaki, R., Schervish, M., Cai, R., Bloss, M., Chan, T., Chen, T., Chen, Q., Chen, X., Chen, Y., Chu, B., Dällenbach, K., Foreback, B., He, X., Heikkinen, L., Jokinen, T., Junninen, H., Kangasluoma, J., Kokkonen, T., Kurppa, M., Lehtipalo, K., Li, H., Li, H., Li, X., Liu, Y., Ma, Q., Paasonen, P., Rantala, P., Pileci, R. E., Rusanen, A., Sarnela, N., Simonen, P., Wang, S., Wang, W., Wang, Y., Xue, M., Yang, G., Yao, L., Zhou, Y., Kujansuu, J., Petäjä, T., Nie, W., Ma, Y., Ge, M., He, H., Donahue, N. M., Worsnop, D. R., Veli-Matti, K., Wang, L., Liu, Y., Zheng, J., Kulmala, M., Jiang, J., and Bianchi, F.: The Synergistic Role of Sulfuric Acid, Bases, and Oxidized Organics Governing New-Particle Formation in Beijing, Geophysical Research Letters, 48, e2020GL091944, https://doi.org/10.1029/2020GL091944, 2021.

Yang, L., Nie, W., Liu, Y., Xu, Z., Xiao, M., Qi, X., Li, Y., Wang, R., Zou, J., Paasonen, P., Yan, C., Xu, Z., Wang, J., Zhou, C., Yuan, J., Sun, J., Chi, X., Kerminen, V.-M., Kulmala, M., and Ding, A.: Toward Building a Physical Proxy for Gas-Phase

https://doi.org/10.5194/acp-2022-565
Preprint. Discussion started: 22 September 2022

Sulfuric Acid Concentration Based on Its Budget Analysis in Polluted Yangtze River Delta, East China, Environmental Science & Technology, 55, 6665-6676, 10.1021/acs.est.1c00738, 2021.

Yao, D., Tang, G., Sun, J., Wang, Y., Yang, Y., Wang, Y., Liu, B., He, H., and Wang, Y.: Annual nonmethane hydrocarbon trends in Beijing from 2000 to 2019, Journal of Environmental Sciences, 112, 210-217, https://doi.org/10.1016/j.jes.2021.04.017, 2022.

Yao, D., Tang, G., Wang, Y., Yang, Y., Wang, L., Chen, T., He, H., and Wang, Y.: Significant contribution of spring northwest transport to volatile organic compounds in Beijing, Journal of Environmental Sciences, 104, 169-181, https://doi.org/10.1016/j.jes.2020.11.023, 2021.

Yao, L., Garmash, O., Bianchi, F., Zheng, J., Yan, C., Kontkanen, J., Junninen, H., Mazon, S. B., Ehn, M., Paasonen, P., Sipila, M., Wang, M. Y., Wang, X. K., Xiao, S., Chen, H. F., Lu, Y. Q., Zhang, B. W., Wang, D. F., Fu, Q. Y., Geng, F. H., Li, L., Wang, H. L., Qiao, L. P., Yang, X., Chen, J. M., Kerminen, V. M., Petaja, T., Worsnop, D. R., Kulmala, M., and Wang, L.: Atmospheric new particle formation from sulfuric acid and amines in a Chinese megacity, Science, 361, 278-+, 10.1126/science.aao4839, 2018.

Yli-Juuti, T., Pajunoja, A., Tikkanen, O.-P., Buchholz, A., Faiola, C., Väisänen, O., Hao, L., Kari, E., Peräkylä, O., Garmash, O., Shiraiwa, M., Ehn, M., Lehtinen, K., and Virtanen, A.: Factors controlling the evaporation of secondary organic aerosol from α-pinene ozonolysis, Geophysical Research Letters, 44, 2562-2570, https://doi.org/10.1002/2016GL072364, 2017.

Yue, D. L., Hu, M., Zhang, R. Y., Wang, Z. B., Zheng, J., Wu, Z. J., Wiedensohler, A., He, L. Y., Huang, X. F., and Zhu, T.: The roles of sulfuric acid in new particle formation and growth in the mega-city of Beijing, Atmospheric Chemistry and Physics, 10, 4953-4960, 10.5194/acp-10-4953-2010, 2010.

Zhang, R., Wang, G., Guo, S., Zamora, M. L., Ying, Q., Lin, Y., Wang, W., Hu, M., and Wang, Y.: Formation of urban fine particulate matter, Chemical Reviews, 115, 3803-3855, 10.1021/acs.chemrev.5b00067, 2015.

Zhang, Y., Vu, T. V., Sun, J., He, J., Shen, X., Lin, W., Zhang, X., Zhong, J., Gao, W., Wang, Y., Fu, T. M., Ma, Y., Li, W., and Shi, Z.: Significant Changes in Chemistry of Fine Particles in Wintertime Beijing from 2007 to 2017: Impact of Clean Air Actions, Environ Sci Technol, 54, 1344-1352, 10.1021/acs.est.9b04678, 2020.

Zhao, J., Du, W., Zhang, Y., Wang, Q., Chen, C., Xu, W., Han, T., Wang, Y., Fu, P., Wang, Z., Li, Z., and Sun, Y.: Insights into aerosol chemistry during the 2015 China Victory Day parade: results from simultaneous measurements at ground level and 260 m in Beijing, Atmospheric Chemistry and Physics, 17, 3215-3232, 10.5194/acp-17-3215-2017, 2017.

Zhao, J., Qiu, Y., Zhou, W., Xu, W., Wang, J., Zhang, Y., Li, L., Xie, C., Wang, Q., Du, W., Worsnop, D. R., Canagaratna, M. R., Zhou, L., Ge, X., Fu, P., Li, J., Wang, Z., Donahue, N. M., and Sun, Y.: Organic Aerosol Processing During Winter Severe Haze Episodes in Beijing, Journal of Geophysical Research: Atmospheres, 124, 10248-10263, 10.1029/2019jd030832, 2019.

Zhao, S., Yin, D., Yu, Y., Kang, S., Qin, D., and Dong, L.: PM2.5 and O3 pollution during 2015–2019 over 367 Chinese cities: Spatiotemporal variations, meteorological and topographical impacts, Environmental Pollution, 264, 114694, https://doi.org/10.1016/j.envpol.2020.114694, 2020.

https://doi.org/10.5194/acp-2022-565
Preprint. Discussion started: 22 September 2022

Zhao, Z., Zhou, Z., Russo, A., Du, H., Xiang, J., Zhang, J., and Zhou, C.: Impact of meteorological conditions at multiple scales on ozone concentration in the Yangtze River Delta, Environmental Science and Pollution Research, 28, 62991-63007, 10.1007/s11356-021-15160-2, 2021.

Zheng, G. J., Duan, F. K., Su, H., Ma, Y. L., Cheng, Y., Zheng, B., Zhang, Q., Huang, T., Kimoto, T., Chang, D., Pöschl, U., Cheng, Y. F., and He, K. B.: Exploring the severe winter haze in Beijing: the impact of synoptic weather, regional transport and heterogeneous reactions, Atmospheric Chemistry and Physics, 15, 2969-2983, 10.5194/acp-15-2969-2015, 2015.

Zhong, J., Zhang, X., Dong, Y., Wang, Y., Liu, C., Wang, J., Zhang, Y., and Che, H.: Feedback effects of boundary-layer meteorological factors on cumulative explosive growth of PM2.5 during winter heavy pollution episodes in Beijing from 2013 to 2016, Atmos. Chem. Phys., 18, 247-258, 10.5194/acp-18-247-2018, 2018.

Zhou, W., Gao, M., He, Y., Wang, Q., Xie, C., Xu, W., Zhao, J., Du, W., Qiu, Y., Lei, L., Fu, P., Wang, Z., Worsnop, D. R., Zhang, Q., and Sun, Y.: Response of aerosol chemistry to clean air action in Beijing, China: Insights from two-year ACSM measurements and model simulations, Environmental pollution, 255, 113345, 10.1016/j.envpol.2019.113345, 2019.

Zhou, Y., Dada, L., Liu, Y., Fu, Y., Kangasluoma, J., Chan, T., Yan, C., Chu, B., Daellenbach, K. R., Bianchi, F., Kokkonen, T. V., Liu, Y., Kujansuu, J., Kerminen, V. M., Petäjä, T., Wang, L., Jiang, J., and Kulmala, M.: Variation of size-segregated particle number concentrations in wintertime Beijing, Atmos. Chem. Phys., 20, 1201-1216, 10.5194/acp-20-1201-2020, 2020.

https://doi.org/10.5194/acp-2022-565
Preprint. Discussion started: 22 September 2022

Atmospheric Chemistry and Physics Discussions

Tables

Table 1. Division of different periods from 2019 to 2022.

Periods of Year-to-Year Variability			Periods of Special Event		
Name	Date	Number of Days	Name	Date	Number of Days
2019	01/01 - 01/22, 2019	22	Reference	02/11 - 02/20, 2019 02/04 - 02/10, 2021 02/18 - 02/20, 2021	20
2020	01/01 - 01/22, 2020	22	COVID	02/04 - 02/20, 2020	17
2021	01/01 - 01/22, 2021	22	Olympics	02/04 - 02/20, 2022	17
2022	01/01 - 01/22, 2022	22	CNY	02/04 - 02/10, 2019 02/11 - 02/17, 2021	14

https://doi.org/10.5194/acp-2022-565
Preprint. Discussion started: 22 September 2022

Figure Legends

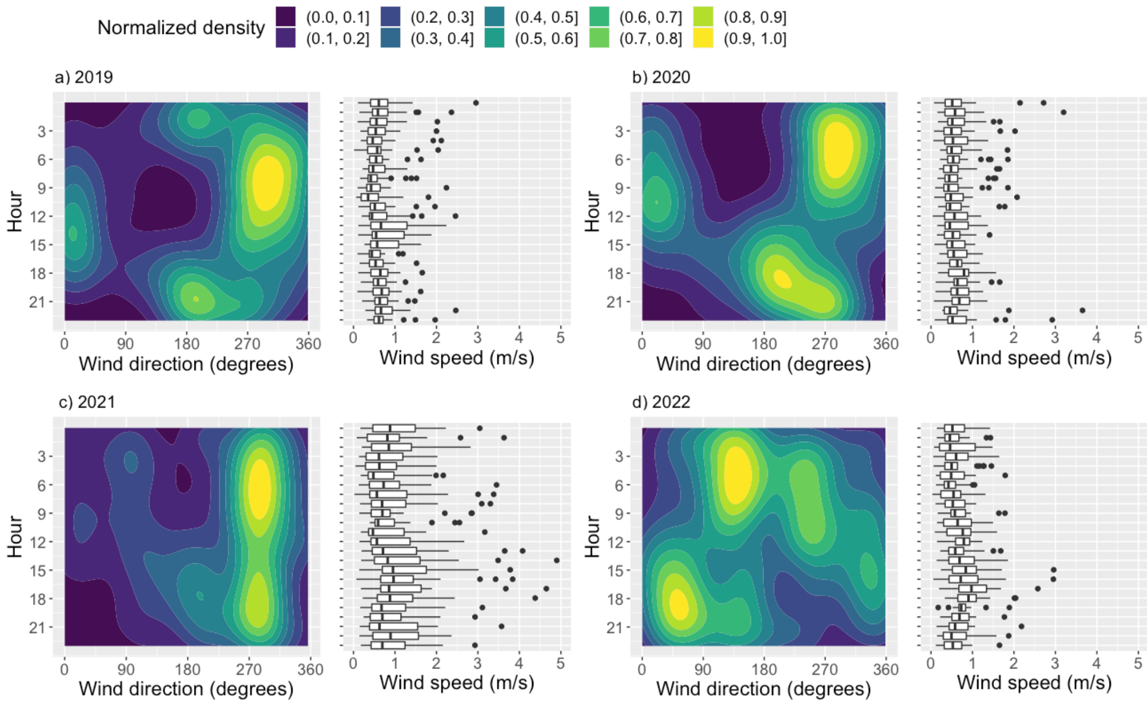

Figure 1. Diurnal variations of wind direction (left panels) and wind speed (right panels) for different years (1st to 22nd January). The wind direction and wind speed are depicted in wind contour plots and boxplots respectively.

https://doi.org/10.5194/acp-2022-565
Preprint. Discussion started: 22 September 2022

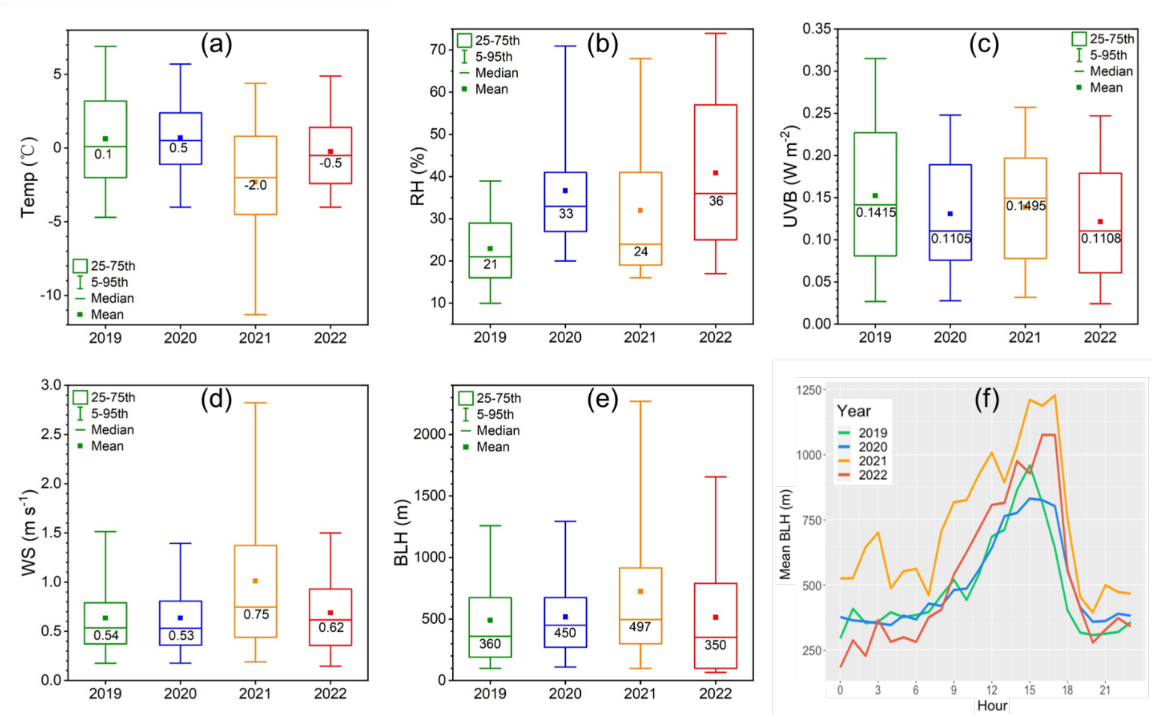

Figure 2. (a) Temperature (Temp), (b) relatively humidity (RH), (c) UVB, (d) wind speed (WS) and (e) boundary layer height (BLH) for different years (1st to 22nd January). (f) Averaged diurnal variations of boundary layer height (BLH) for different years (1st to 22nd January). The value inside each box is the median value of corresponding parameter. Please note that for UVB, only daytime (08:00 – 16:00) dataset was used.

https://doi.org/10.5194/acp-2022-565
Preprint. Discussion started: 22 September 2022

Atmospheric Chemistry and Physics
Open Access
Discussions

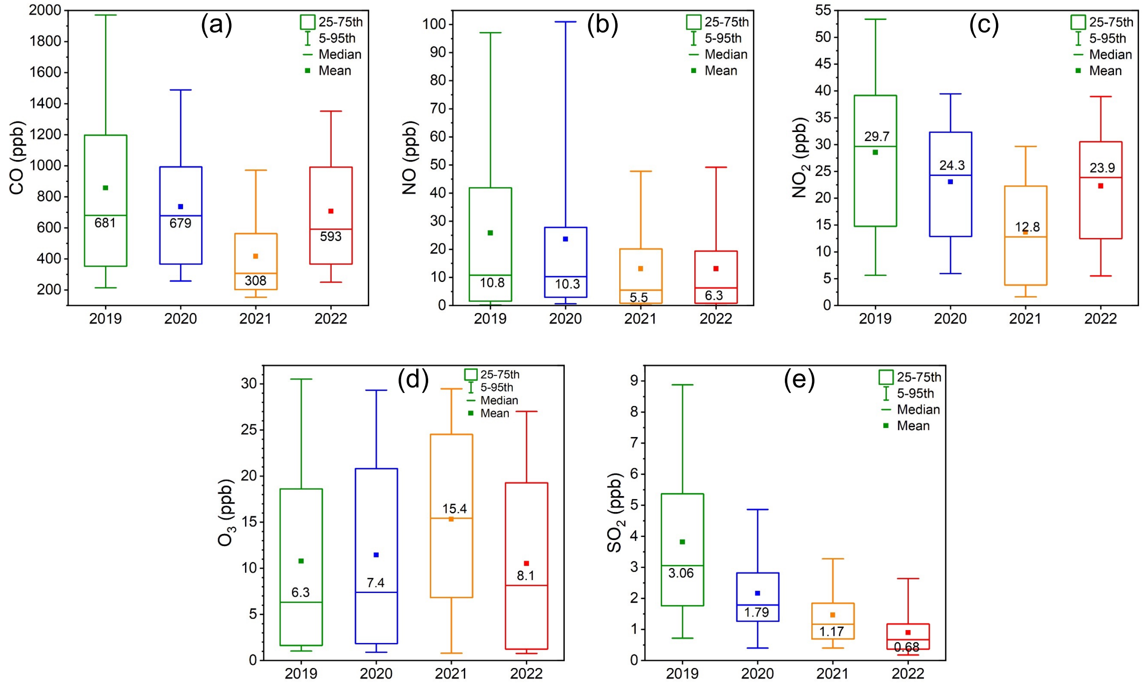

Figure 3. Mixing ratios of (a) CO, (b) NO, (c) NO_2, (d) O_3 and (e) SO_2 for different years (1st to 22nd January). The value inside each box is the median value of corresponding parameter.

https://doi.org/10.5194/acp-2022-565
Preprint. Discussion started: 22 September 2022

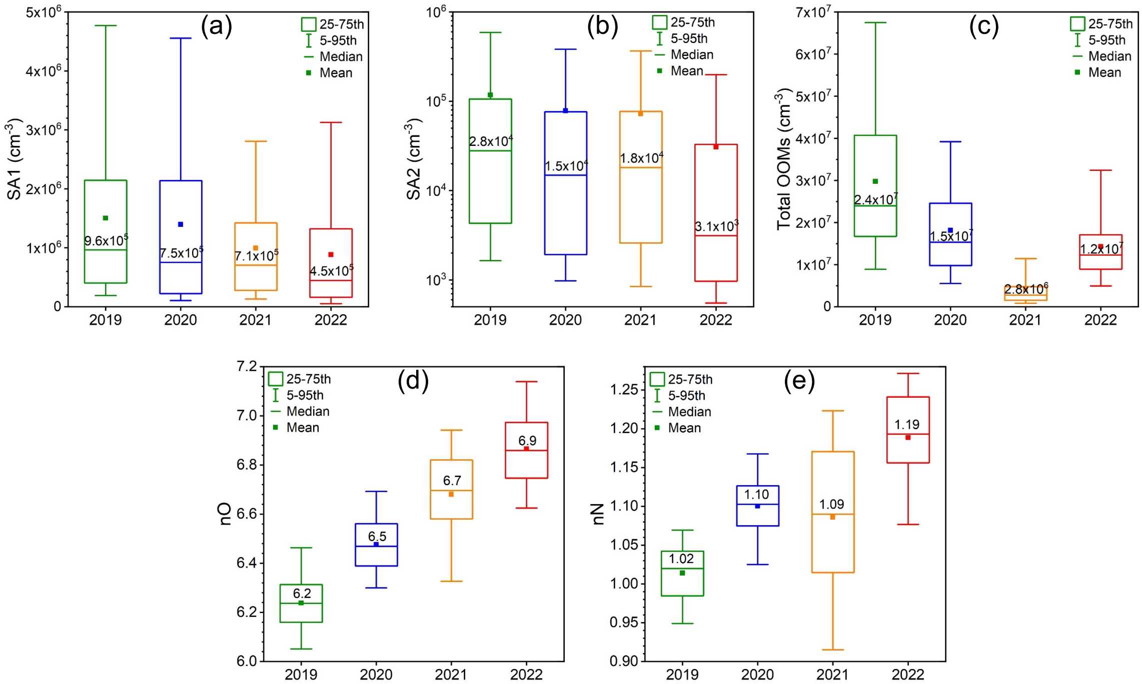

860 **Figure 4**. (a) Concentration of sulfuric acid monomer (SA1), (b) concentration of sulfuric acid dimer (SA2), (c) concentration of total OOMs, (d) fraction weighted oxygen number of OOMs (nO), and (e) fraction weighted nitrogen number of OOMs (nN) for different years (1st to 22nd January). The value inside each box is the median value of corresponding parameter.

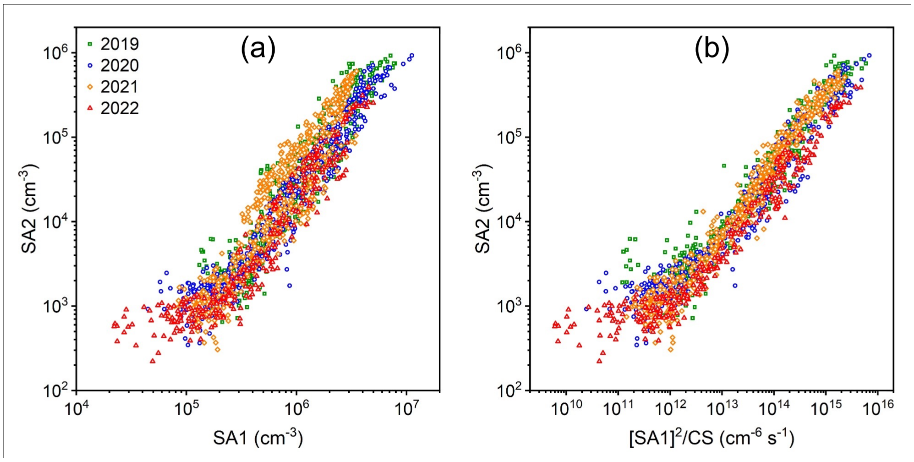

865 **Figure 5**. Sulfuric acid dimer (SA2) vs. (a) sulfuric acid monomer (SA1) and (b) $[SA1]^2/CS$ from 2019 to 2022 (1st to 22nd January).

https://doi.org/10.5194/acp-2022-565
Preprint. Discussion started: 22 September 2022

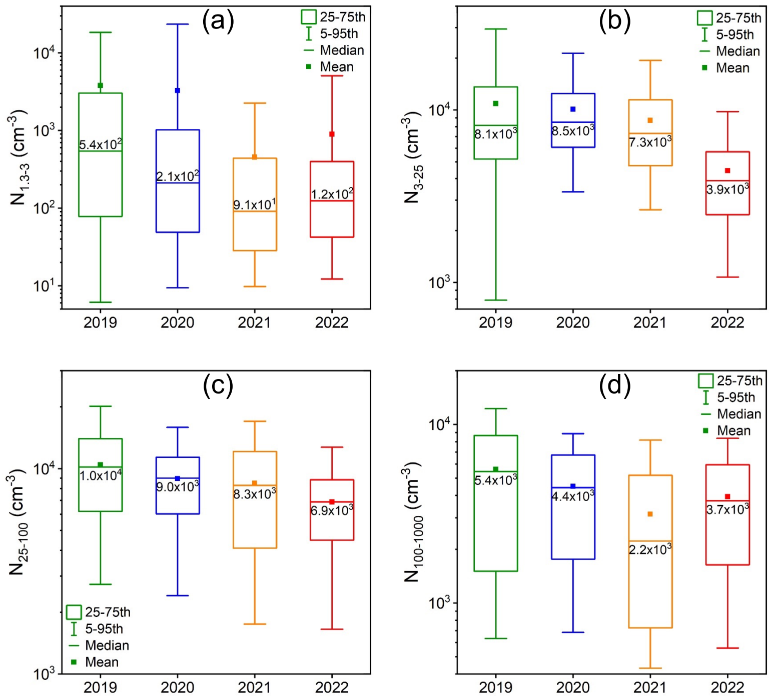

Figure 6. Number concentration of (a) sub-3 nm aerosols ($N_{1.3\text{-}3}$), (b) 3-25 nm aerosols ($N_{3\text{-}25}$), (c) 25-100 nm aerosols ($N_{25\text{-}100}$) and (d) 100-1000 nm aerosols ($N_{100\text{-}1000}$) for different years (1st to 22nd January). The bottom and top edges of the boxes indicate the 25th and 75th percentiles, respectively. The horizontal lines inside the boxes represent the median values. The red cross markers denote the outliers.

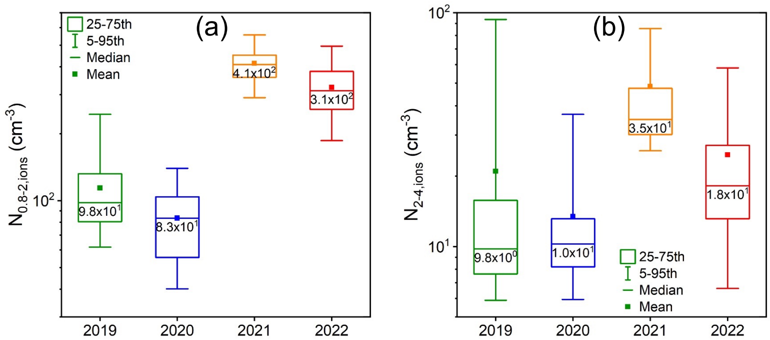

Figure 7. Number concentration of (a) 0.8-2 nm ($N_{0.8\text{-}2,\ \mathrm{ions}}$) and (b) 2-4 nm ($N_{2\text{-}4,\ \mathrm{ions}}$) positive ions measured by NAIS for different years (1st to 22nd January). The y-axis range is the same in each figure. The bottom and top edges of the boxes indicate the 25th and 75th percentiles, respectively. The horizontal lines inside the boxes represent the median values. The red cross markers denote the outliers.

https://doi.org/10.5194/acp-2022-565
Preprint. Discussion started: 22 September 2022

Atmospheric Chemistry and Physics Discussions

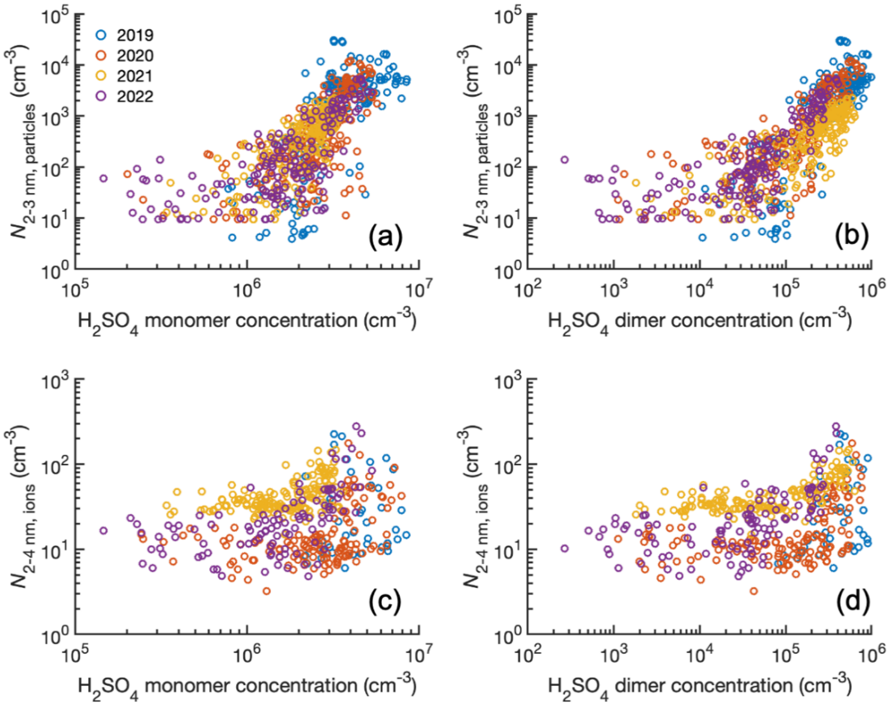

880 **Figure 8.** The relations (a) between particle number concentration in 2-3 nm size range and H_2SO_4 monomer concentration, (b) between particle number concentration in 2-3 nm size range and H_2SO_4 dimer concentration, (c) between ion number concentration in 2-4 nm size range and H_2SO_4 monomer concentration and (d) between ion number concentration in 2-4 nm size range and H_2SO_4 dimer concentration for different years (1st to 22nd January).

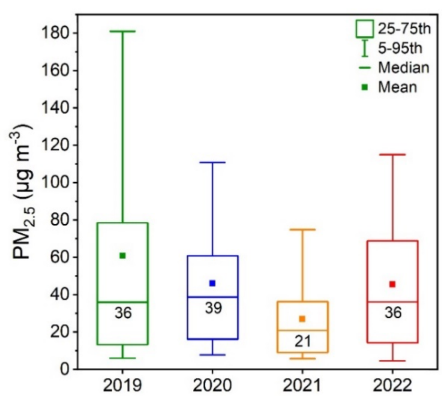

885

Figure 9. $PM_{2.5}$ mass concentration for different years (1st to 22nd January). The bottom and top edges of the boxes indicate the 25th and 75th percentiles, respectively. The horizontal lines inside the boxes represent the median values. The dots denote the mean values.

https://doi.org/10.5194/acp-2022-565
Preprint. Discussion started: 22 September 2022

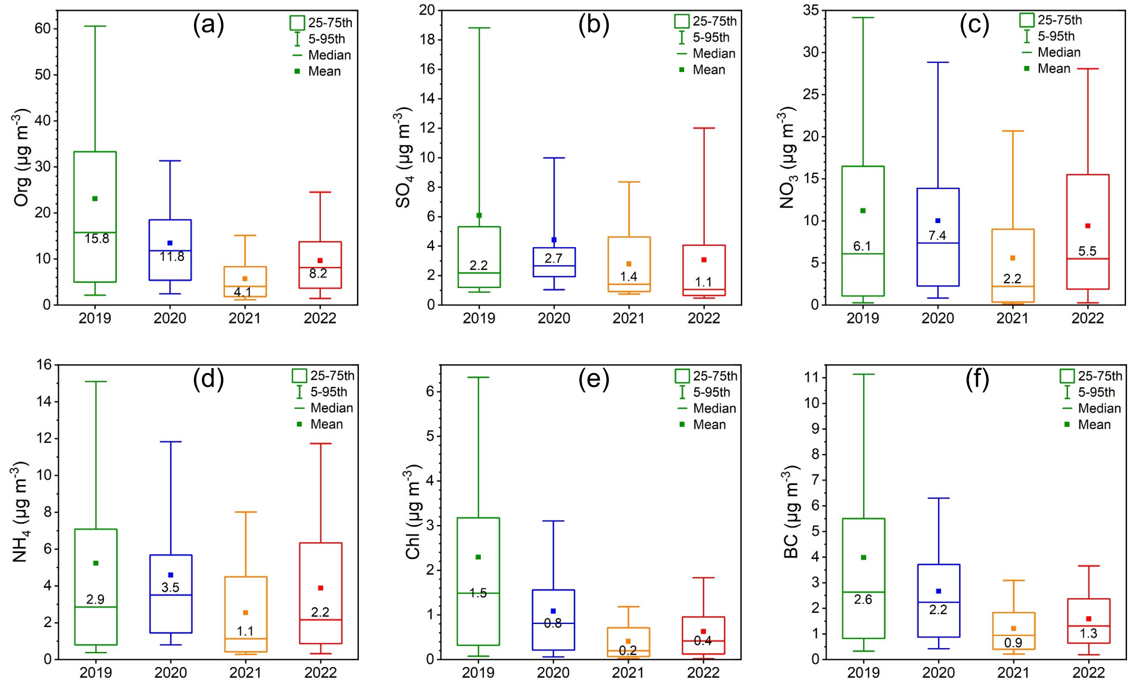

Figure 10. Mass concentrations of $PM_{2.5}$ compositions including (a) organics (Org), (b) sulfate (SO_4), (c) nitrate (NO_3), (d) ammonium (NH_4), (e) chloride (Chl), and (f) black carbon (BC) for different years (1st to 22nd January). The bottom and top edges indicate the 25th and 75th percentiles, respectively. the circles denote the median values.

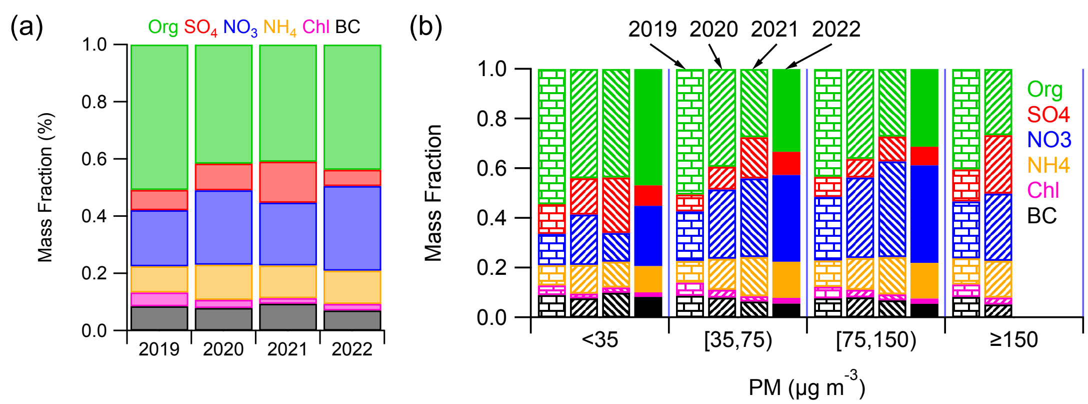

Figure 11. Contributions of $PM_{2.5}$ compositions including organics (Org), sulfate (SO_4), nitrate (NO_3), ammonium (NH_4), chloride (Chl), and black carbon (BC) (a) for different years (1st to 22nd January), and (b) under different $PM_{2.5}$ levels.

https://doi.org/10.5194/acp-2022-565
Preprint. Discussion started: 22 September 2022

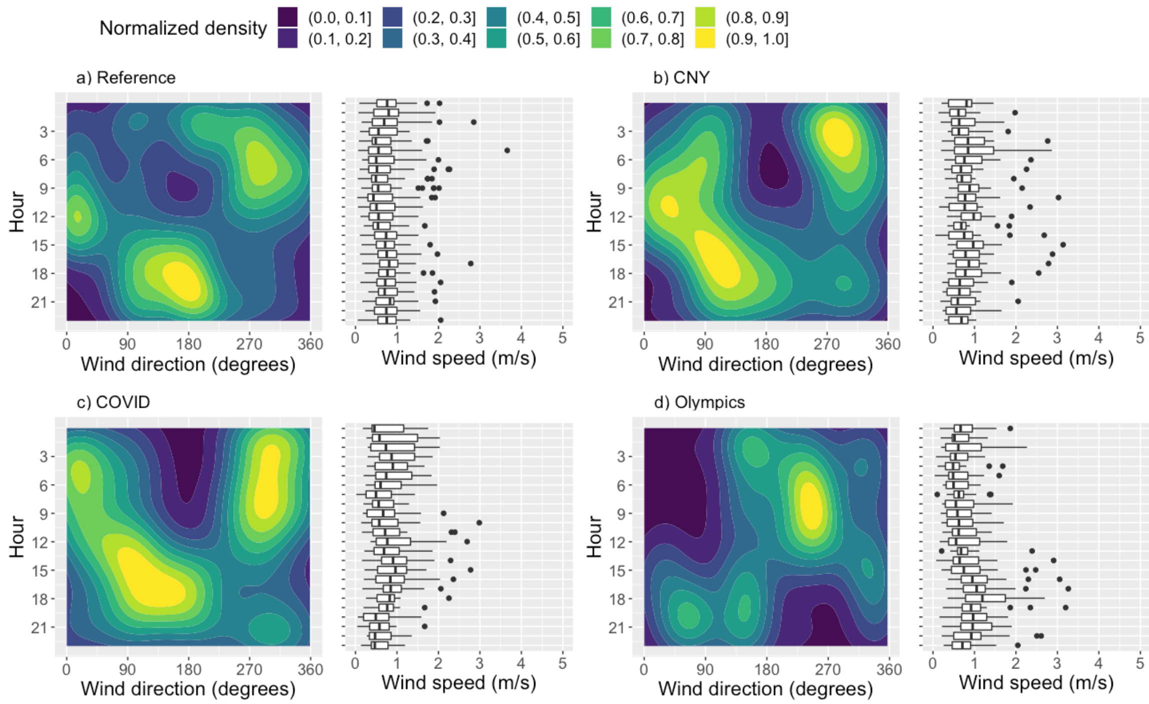

900 **Figure 12.** Diurnal variations of wind direction (left panels) and wind speed (right panels) for reference, COVID, Olympics and CNY periods. The wind direction and wind speed are depicted in wind contour plots and boxplots respectively.

https://doi.org/10.5194/acp-2022-565
Preprint. Discussion started: 22 September 2022

Atmospheric Chemistry and Physics Discussions

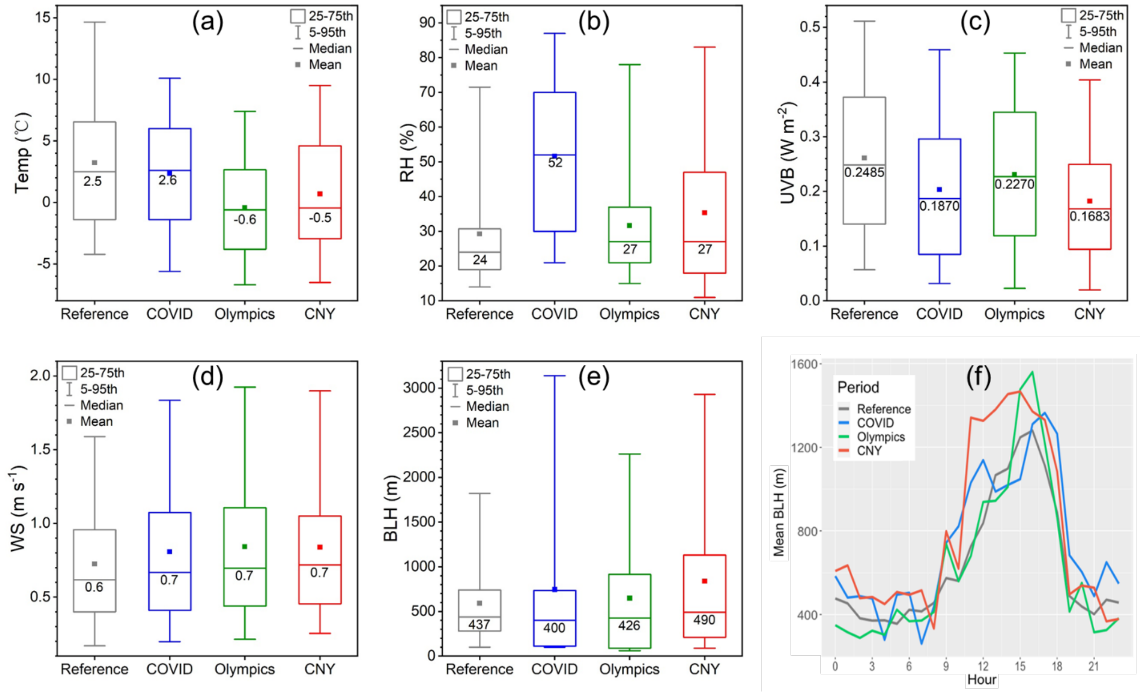

905 **Figure 13.** (a) Temperature (Temp), (b) relatively humidity (RH), (c) UVB, (d) wind speed (WS) and (e) boundary layer height (BLH) for reference, COVID, Olympics and CNY periods. (f) Averaged diurnal variations of boundary layer height (BLH) for reference, COVID, Olympics and CNY periods. The value inside each box is the median value of corresponding parameter. Please note that for UVB, only daytime (08:00 – 16:00) dataset was used.

Atmospheric Chemistry and Physics
Open Access
EGU
Discussions

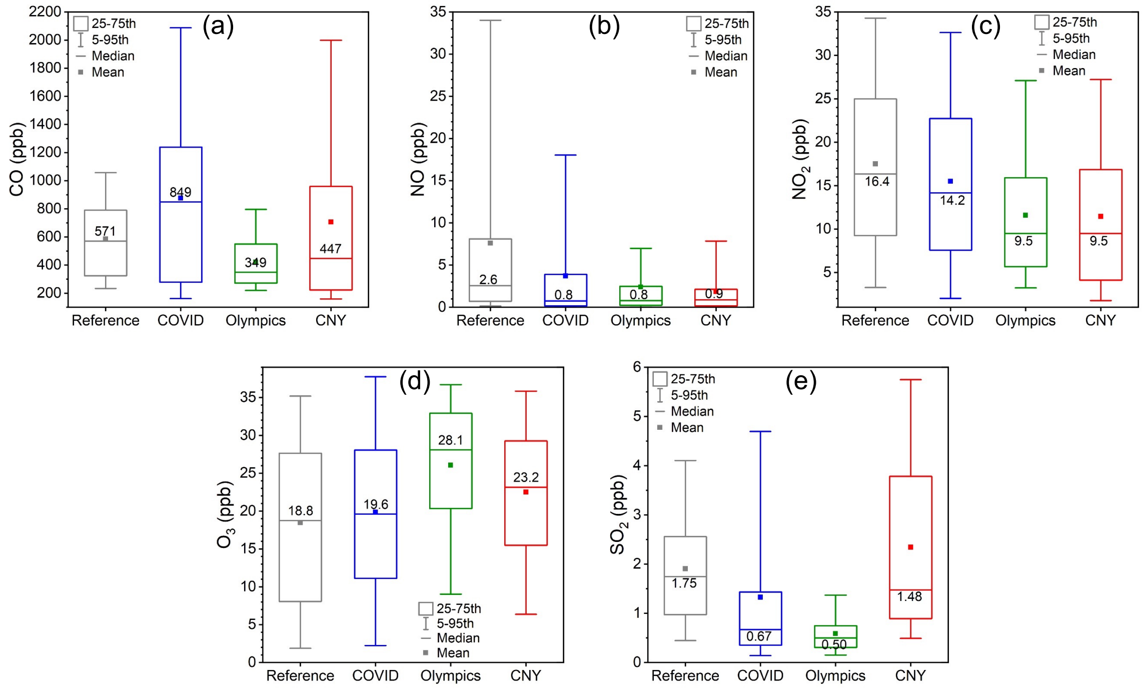

910 **Figure 14**. Mixing ratios of (a) CO, (b) NO, (c) NO_2, (d) O_3 and (e) SO_2 for reference, COVID, Olympics and CNY periods. The value inside each box is the median value of corresponding parameter.

Atmospheric Chemistry and Physics Discussions

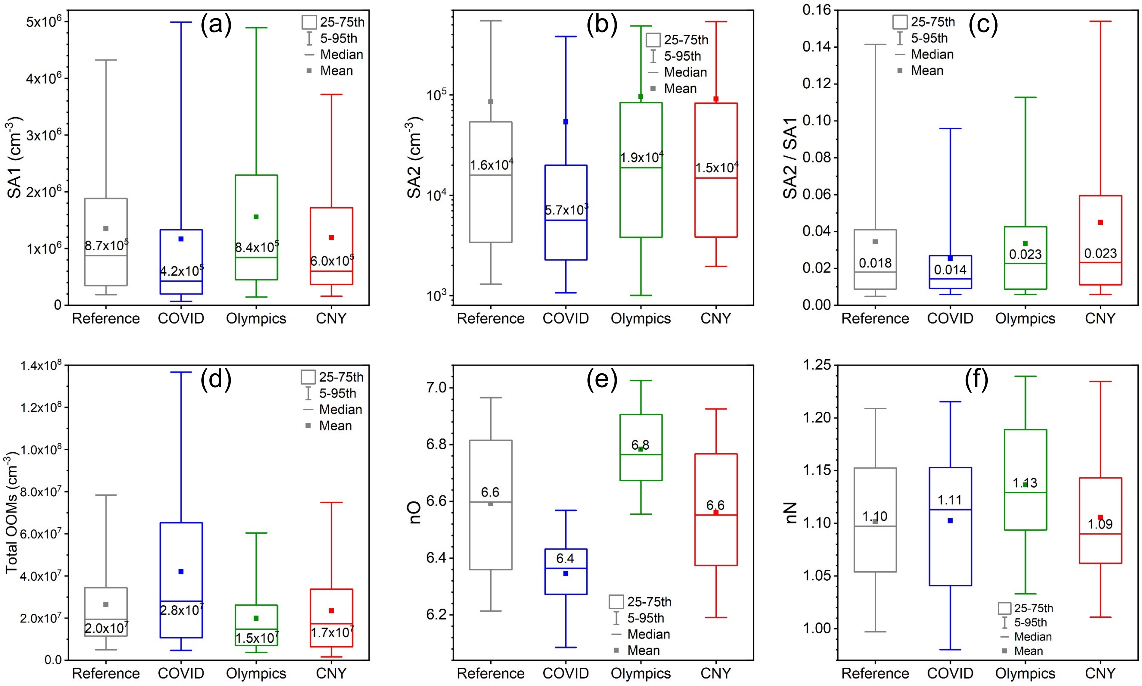

Figure 15. (a) Concentration of sulfuric acid monomer (SA1), (b) concentration of sulfuric acid dimer (SA2), (c) ratio of SA2 to SA1, (d) concentration of total OOMs, (e) fraction weighted oxygen number of OOMs (nO), and (f) fraction weighted nitrogen number of OOMs (nN) for reference, COVID, Olympics and CNY periods. The value inside each box is the median value of corresponding parameter.

https://doi.org/10.5194/acp-2022-565
Preprint. Discussion started: 22 September 2022

Atmospheric Chemistry and Physics
Discussions

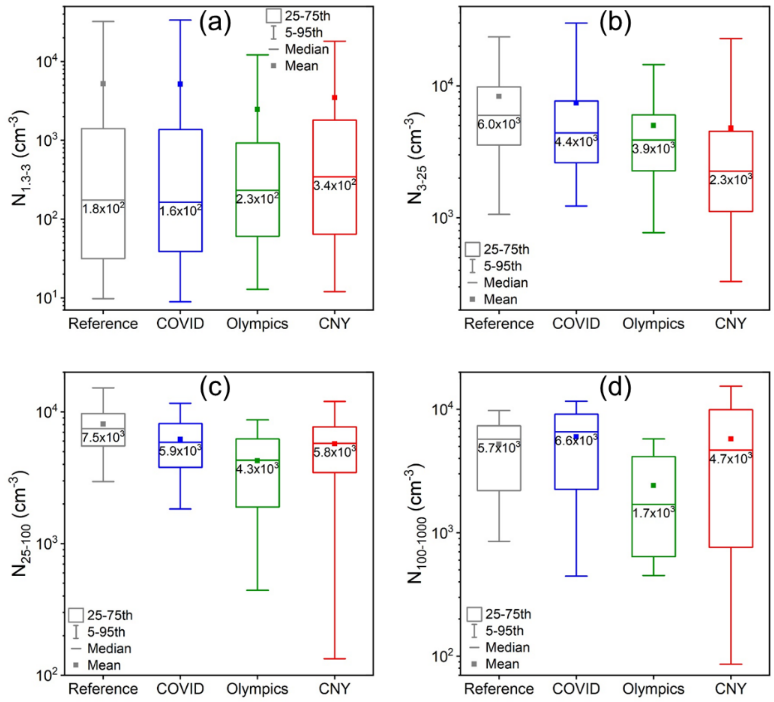

Figure 16. Comparisons of number concentration of (a) sub-3 nm aerosols ($N_{1.3\text{-}3}$), (b) 3-25 nm aerosols ($N_{3\text{-}25}$), (c) 25-100 nm aerosols ($N_{25\text{-}100}$) and (d) 100-1000 nm aerosols ($N_{100\text{-}1000}$) for reference, COVID, Olympics and CNY periods. The bottom and top edges of the boxes indicate the 25th and 75th percentiles, respectively. The horizontal lines in the boxes represent the median values. The red cross markers denote the outliers.

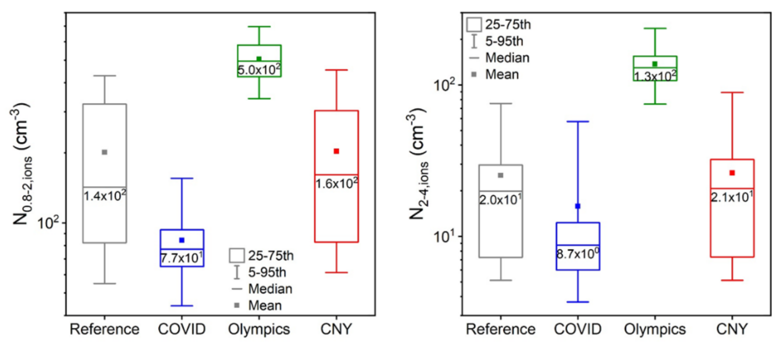

Figure 17. Comparisons of number concentration of (a) 0.8-2 nm ($N_{0.8\text{-}2}$) and (b) 2-4 nm ions ($N_{2\text{-}4}$) for reference, COVID, Olympics and CNY periods. The bottom and top edges of the boxes indicate the 25th and 75th percentiles, respectively. The horizontal lines in the boxes represent the median values. The red cross markers denote the outliers.

https://doi.org/10.5194/acp-2022-565
Preprint. Discussion started: 22 September 2022

Atmospheric Chemistry and Physics
Discussions

930

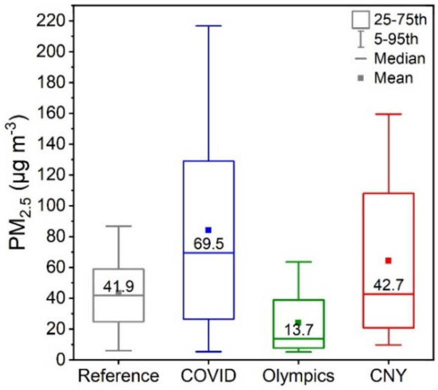

Figure 18. $PM_{2.5}$ mass concentration for reference, COVID, Olympics and CNY periods. The bottom and top edges of the boxes indicate the 25th and 75th percentiles, respectively. The horizontal lines inside the boxes represent the median values. The dots denote the mean values.

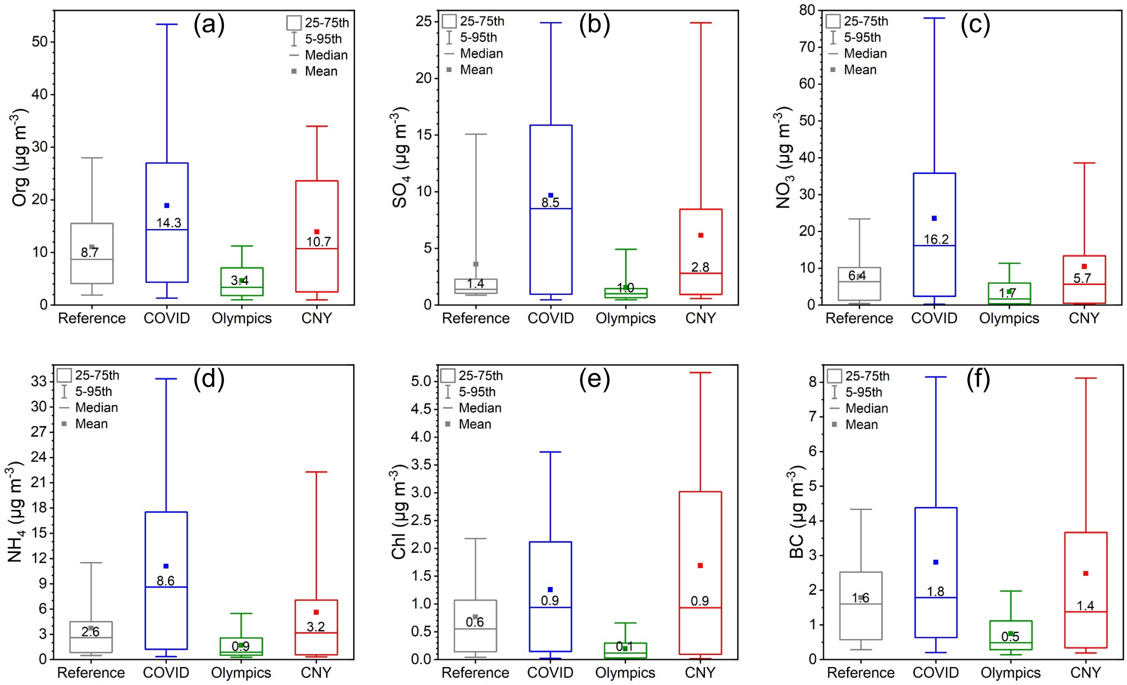

935 **Figure 19.** Mass concentrations of $PM_{2.5}$ compositions including (a) organics (Org), (b) sulfate (SO_4), (c) nitrate (NO_3), (d) ammonium (NH_4), (e) chloride (Chl), and (f) black carbon (BC) for reference, COVID, Olympics and CNY periods. The median values (cycle) and 25th and 75th percentiles (horizontal error bars) are shown.

https://doi.org/10.5194/acp-2022-565
Preprint. Discussion started: 22 September 2022

Atmospheric Chemistry and Physics Discussions

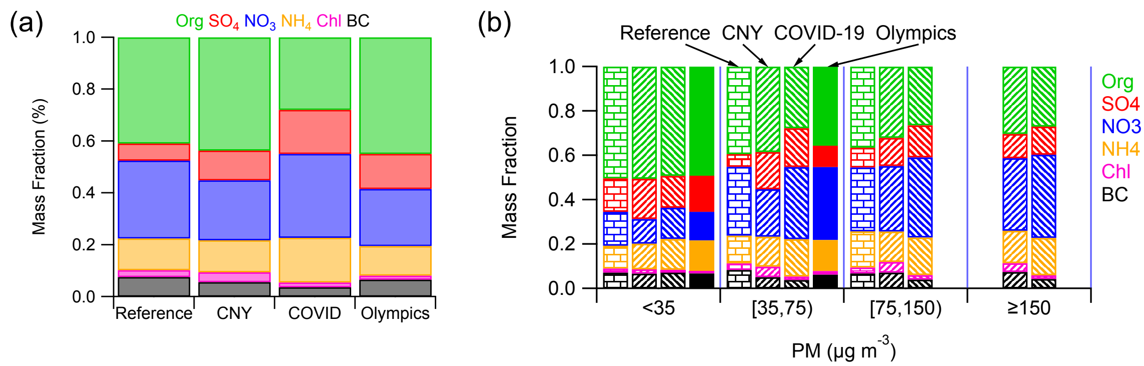

940 **Figure 20.** Contributions of $PM_{2.5}$ compositions including organics (Org), sulfate (SO_4), nitrate (NO_3), ammonium (NH_4), chloride (Chl), and black carbon (BC) (a) for reference, COVID, Olympics and CNY periods, and (b) under different $PM_{2.5}$ levels.